University of Wollongong

Research Online

Faculty of Engineering and Information Sciences - Papers: Part A

Faculty of Engineering and Information Sciences

1-1-2016

Response of piles subjected to progressive soil movement

Hongyu Qin
Flinders University

Wei Dong Guo
University of Wollongong, wdguo@uow.edu.au

Recommended Citation

Qin, Hongyu and Guo, Wei Dong, "Response of piles subjected to progressive soil movement" (2016). *Faculty of Engineering and Information Sciences - Papers: Part A*. 5857.
https://ro.uow.edu.au/eispapers/5857

Response of piles subjected to progressive soil movement

Abstract

Model tests were conducted to investigate the behavior of vertically loaded, free head piles undergoing lateral soil movement using an experimental apparatus developed in house. This paper presents ten new tests on an instrumented model pile in dry sand, which provide the profiles of bending moment, shear force and pile deflection along the pile, the development of maximum bending moment Mmax, maximum shear force Tmax, and pile deflection y0 at the ground surface with soil movement. The tests reveal the effects of axial load P (at pile head), the distance between the tested pile and source of free soil movement Sb, sliding depths, and angle of soil movement (via loading angle) on the pile response. For instance, the axial loading P leads to extra bending moment and deflection in the passive pile; the Mmax reduces with increase in Sb; and the Mmax is proportional to the "angle" of soil movement. The elastic solution by Guo and Qin [Guo, W. D., Qin, H. Y., 2010, "Thrust and Bending Moment of Rigid Piles Subjected to Moving Soil," Can. Geotech. J., Vol. 47, No. 2, pp. 180-196] was used to predict the development of Mmax and Tmax observed in the current tests, a boundary element analysis, and an in situ pile test, respectively. It provides satisfactory predictions for all cases against the measured data.

Keywords

piles, response, movement, soil, progressive, subjected

Disciplines

Engineering | Science and Technology Studies

Publication Details

Qin, H. & Guo, W. (2016). Response of piles subjected to progressive soil movement. Geotechnical Testing Journal, 39 (1), 106-125.

RESPONSE OF PILES SUBJECTED TO PROGRESSIVE SOIL MOVEMENT

Hongyu Qin[1] and Wei Dong Guo[*2]

[1]Hongyu Qin

School of Computer Science, Engineering and Mathematics
Flinders University
GPO Box 2100
SA 5001
Australia
TEL: 61-8-8201 2763
FAX: 61-8-8201 2904
Email: **hongyu.qin@Flinders.edu.au**

[2]*Wei Dong Guo

Corresponding author
School of Civil, Mining and Environmental Engineering
University of Wollongong
NSW 2522
Australia
TEL: 61-2-42213036
Email: **wdguo@uow.edu.au**

Number of words: 6367
Number of tables: 3
Number of figures: 16

Abstract

Model tests were conducted to investigate the behavior of vertically loaded, free head piles undergoing lateral soil movement using an experimental apparatus developed in house. This paper presents ten new tests on an instrumented model pile in dry sand, which provide the profiles of bending moment, shear force and pile deflection along the pile, the development of maximum bending moment M_{max}, maximum shear force T_{max}, and pile deflection y_0 at the ground surface with soil movement. The tests reveal the effects of axial load P (at pile head), the distance between the tested pile and source of free soil movement S_b, sliding depths, and angle of soil movement (via loading angle) on the pile response. For instance, the axial loading P leads to extra bending moment and deflection in the passive pile; the M_{max} reduces with increase in S_b; and the M_{max} is proportional to the 'angle' of soil movement. The elastic solution by Guo and Qin (2010) was used to predict the development of M_{max} and T_{max} observed in the current tests, a boundary element analysis, and an in-situ pile test, respectively. It provides satisfactory predictions for all cases against the measured data.

Key words: Laboratory tests, piles, axial loading, lateral soil movement, soil-pile interaction

1. Introduction

Piles may be subjected to lateral soil movements when used to increase slope stability, to support bridge abutment, or used as foundations of tall buildings adjacent to tunneling or excavation. The soil movements may induce additional internal force and deflection in the piles (called passive piles), which may adversely affect the serviceability of the superstructure or even compromise the structural integrity of the piles in extreme conditions. Response of the piles has been extensively studied through centrifuge modeling and 1g small scale model tests (Stewart et al., 1994, Bransby and Springman, 1997, Leung et al., 2000, 2003, 2006, Ong et al., 2006, 2009, Poulos et al., 1995, Chen et al., 1997, Ellis and Springman, 2001, Pan et al., 2000, 2002, White et al., 2008, Fioravante, 2008, Yoon and Ellis, 2009, Guo and Qin, 2010, Suleiman et al., 2014), field monitoring (Smethurst and Powrie, 2007, Frank and Pouget, 2008, O'Kelly et al., 2008, Lirer, 2012), and theoretical and numerical analysis (Poulos, 1973, 1995, De Beer, 1977, Ito and Matsui, 1975, Fukouka, 1977, Viggiani, 1981, Reese et al., 1992, Chow, 1996, Chen and Poulos, 1997, Cai and Ugai, 2000, 2003, 2011, Chen and Martin, 2002, Chmoulian, 2004, Liang and Yamin, 2009, Ellis et al., 2010, Guo, 2013, 2014a, 2014b, Ashour and Ardalan, 2012, Kanagasbai et al., 2011, Pan et al., 2012, Galli and di Prisco, 2013, Muraro et al., 2014).

Physical modelling using small scale tests has brought valuable insights into the complex, three-dimensional mechanisms of pile-soil interaction. They help to clarify and quantify key parameters, develop conceptual models, assess the applicability of analytical models (Randolph and House, 2001). Dimensional analysis enables the key variables controlling the problem to be determined (Byrne, 2014), from which the scalability of 1g model can be judged.

To investigate the response of vertically loaded piles and pile groups subjected to lateral soil movements, Guo and Ghee (2004) developed a new experimental apparatus. The team conducted a large number of tests on piles in sand, as partially published, for example, by Guo and Ghee (2004, 2005), Guo et al. (2006), Guo and Qin (2005, 2006, 2010), and Qin and Guo (2010a, 2010b). Among them, Guo and Qin

(2010) present 14 typical model pile tests in moving sand concerning two diameters, two vertical pile loading levels and varying sliding depths imposed by a triangular loading block. They developed a simple solution to estimate the development of maximum bending moment and maximum shear force induced in the piles with soil movement. They further provided successful predictions of the ratio of the moment and the shear force observed in eight in-situ test piles and one centrifuge test pile subjected to soil movement. The solution is also validated by Qin and Guo (2010a, 2010b) for a uniform movement profile.

The theoretical and numerical analysis, on the other hand, can be broadly classified into four categories (Stewart et al., 1994): (1) empirical methods; (2) pressure-based methods; (3) displacement-based methods; and (4) numerical methods of finite element and finite difference analysis, etc. The pressure-based methods (Ito and Matsui, 1975, Viggiani, 1981, Chmoulian, 2004) are proposed to estimate the ultimate lateral resistance of slope stabilizing piles. They cannot simulate the pile response which depends on both pile-soil interaction modes and their relative displacements (Guo, 2013, Smethurst and Powrie, 2007, White et al., 2008, Dobry et al., 2003; Brandenberg et al., 2005). The displacement-based methods allow incorporating the soil displacements around the pile (rather than the frame movement presented in this paper later), pile-soil interaction and their relative displacements. This is done by estimating the free-field lateral soil movement (in the absence of piles), and pile responses (by superimposing the soil movements). The methods include subgrade reaction approach (including the p ~ y analysis) (Fukouka, 1977, Byrne et al., 1984, Cai and Ugai, 2003, 2011, Reese et al., 1992, Suleiman et al., 2007, Frank and Pouget, 2008, White et al., 2008); and continuum approach (Poulos, 1973, 1995). Three-dimensional numerical analysis (using finite element and finite difference methods) is rigorous, and powerful in capturing behaviour of passive piles, and in considering impact of soil stratigraphy, non-linear behavior, and movement profiles, and pile-soil interaction and pile-pile interaction. These methods are useful, but are computational expensive, time-consuming and depend on input parameters.

The pile-soil interaction mechanism for passive piles is not yet clearly understood.

Using numerical simulation, for instance, Kanagasbai et al. (2011) and Kourkoulis et al. (2011, 2012) enforced a fixed depth of uniform movement at the boundary of the mesh domain to mimic soil translation. This is different from progressive soil movement (laterally and vertically) in a practical scenario, as is evident during deep excavations (Leung et al., 2000, 2003), embankment loading (Ellis and Springman, 2001), or close to embedded retaining walls in a foundation pit (Yap and Pound, 2003, Katzenbach et al., 2005). As for physical modeling, limited field and laboratory data are available on response of the piles to (1) the distance between source of soil movement and pile location, (2) combined lateral soil movement and axial loading, and (3) soil movement 'angle'.

This study provides further in-depth experimental investigation into the response of vertically loaded free head single piles subjected to lateral soil movement. For four series, ten new model tests were conducted on instrumented piles in progressively moving sand, to obtain bending moment, shear force and deflection profiles along the pile and the development of maximum bending moment, maximum shear force and pile deflection at model ground surface against frame movement. This paper aims to:

- Quantify the responses of piles in progressively moving sand using the test results of instrumented piles;
- Examine the effect of the distance between the test pile and source of free soil movement, axial load level, sliding depth, and angle of soil movement on the pile response; and
- Further validate the elastic solution by Guo and Qin (2010) using the new tests, a boundary element analysis, and an in-situ pile test.

2. Apparatus and test procedures

2.1 Shear box and loading system

Fig. 1 shows a test setup, a schematic cross section of the shear box, and the loading system. The inner dimensions of the shear box are 1.0 m both in length and width and 0.8 m in height. The upper part of the shear box consists of a series of 25 mm thick stacked square laminar steel frames. The frames, which are allowed to slide, contain the "moving sand layer" of thickness L_m. The lower section of the shear box comprises a 400 mm height fixed timber box and the desired number of laminar steel frames, so that a "stable sand layer" of thickness L_s (≥400 mm) can be enforced. By changing the number of frames in the upper and lower parts in the shear box, the depths of the stable layer and moving layer are varied accordingly. Note that the L_m and L_s are defined at the loading location. They are unknown around a test pile at a distance of S_b, due to their variations across the shear box.

The loading system includes a hydraulic jack (which is connected with a triangular loading block that is placed on the upper movable laminar frames), and some weights on top of the test pile. The 'triangular' loading block was made to an angle of 15°, 22.5° and 30°, respectively (see Fig. 2). Pumping the hydraulic jack pushes the loading block and the upper frames to slide horizontally, and generates the soil movements in the shear box. This advancement also gradually mobilizes the lower frames, rendering increase in the sliding depth. The frame movement w_f is measured from the reference board shown in Fig. 1(d). Using the block 1 (θ=15°), for instance, the sliding depth at a lateral w_f is equal to $3.33w_f$, until it reaches a pre-specified final depth of L_m (Guo and Qin, 2010). Thereafter, any additional increase in w_f results in additional uniform movement or an overall trapezoid soil movement. To simulate free head condition, vertical load was exerted by placing a desired number of weights on the pile head, which are secured by a sling fasten from the overhead bridge.

Response of the pile is monitored via ten pairs of strain gauges distributed along the pile and two dial gauges above the model ground. The test readings were recorded and processed via a data acquisition system and a computer, which are transferred into 'measured' pile response using a purposely designed program discussed later.

2.2. Instrumentation and model pile

Fig. 3 shows a schematic diagram of the instrumented model pipe pile used in the tests. The aluminum pile has a length of 1200 mm, an outer diameter of 32 mm and a wall thickness of 1.5 mm. Its surface was instrumented with strain gauges at an interval of 100 mm, and subsequently covered with 1 mm of epoxy and wrapped with electrical tapes to protect from damage. The gauges were calibrated prior to the tests (Guo and Qin 2010). Their readings were converted to actual strains using calibration factor for each gauge. Two dial gauges were set up to measure the pile deflections above the model ground surface. Their readings and the distance between the gauges allow the transverse pile deflections and rotation at the ground surface to be calculated, which act as the boundary conditions for calculating deflection profile.

2.3 Model sand ground properties

Medium oven-dried quartz sand was used in this study. The sand has an effective particle size D_{10} of 0.12 mm, a uniformity coefficient C_u of 2.9 and a coefficient of curvature C_c of 1.15, respectively. The sand was discharged (from a sand rainer) into the shear box at a falling height of 600 mm. This generates a reasonably uniform model ground with a dry unit weight of 16.27 kN/m^3 and a relative density D_r of 89%. The sand has a peak angle of internal friction of 38º as measured from three sets of direct shear tests at a normal stress of 26.7 kPa through 67.6 kPa (Ghee, 2010).

2.4. Test program

Twelve typical tests on the model pile were conducted to investigate the effect of distance between the free soil movement source and the test pile, S_b, axial load level, P, sliding depth, L_m, and loading block angle, θ. As with previous notation, each test is denoted by one to two letters and a few numbers, indicating “loading block shape”, “moving soil depth”, “pile diameter”, and “axial load”, e.g. TS32-0: (i) “T” signifies the triangular loading block; (ii) “S” refers to a predetermined sand sliding depth of L_m = 200 mm; (iii) “32” indicates 32 mm in pile diameter; and (iv) “0” represents an axial load of 0 N. If unspecified, the pile was always installed in the center of the shear box, i.e. S_b = 500 mm. The tests are detailed in Table 1 and described below.

(1) TS32-0 and TS32-294 (as reported previously by Guo and Qin (2010)): The pile was installed at the center of the shear box and conducted under a predetermined final sliding layer depth of L_m = 200 mm (with a stable layer L_s = 500 mm) with 0 N and 294 N axial load, respectively. Test TS32-0 was taken as the 'standard test' for comparison, from which a parameter is varied in the rest tests. Specifically,

(2) TS32-0-340 and TS32-0-660 installed at a distance S_b of 340 mm and 660 mm (series 1).

(3) TS32-588 and TS32-735 with an axial load P = 588 N and P = 735 N (series 2).

(4) T32-0 (L_m=125), T32-0 (L_m=250), T32-0 (L_m=300), T32-0 (L_m=350) with a predetermined sliding depth L_m=125, 250, 300, 350 mm, respectively (series 3).

(5) TS32-0 (θ=22.5°) and TS32-0 (θ=30°) with the loading block 2 (θ=22.5°) and 3 (θ=30°) (series 4). Note the tests in series 1, 2 and 3 were all conducted using the loading block 1 (θ=15°) (see Fig. 2).

3. Test results

The discrete measured strains need to be fitted by a continuous analytical function, to gain bending moment distribution along the pile length. Fifth or sixth order polynomial functions (Bransby and Springman, 1997; Chen 1994), and fourth or fifth order spline functions (Smethurst and Powrie, 2007, Frank and Pouget, 2008) were adopted, due to easy to integrate and differentiate. However, it is difficult to apply the technique of polynomial curve fitting to the discrete bending moments in the current model tests. An accurate fit to the moment profiles, for instance, of test TS32-588 (see Fig 4(a)) at $w_f \geq 50$ mm requires fourth to sixth order polynomial, which still result in inconsistence at various frame movements. From linear elastic beam theory, numerical integration and differential were thus used to derive the pile rotation, displacement, shear force, and soil reaction (net force per unit length on the pile).

The bending moment profile was firstly obtained from the stain gauge readings. They were integrated numerically (using the trapezoidal rule) to compute the pile rotation profiles (incorporating the measured rotation at ground surface); and the rotation profiles were in turn integrated to offer the pile displacements (considering the displacement at ground surface).

Double differential of discrete bending moment data points is reported to amplify measurement errors and renders an inaccurate soil reaction. Presently, there is no generally accepted standard method for deducing the soil reaction. Levachev et al. (2002) proposed to use a cubic polynomial (by least squares) to fit five successive sets of equally spaced measured bending moment data, which is then differentiated at the central point. The method offers more reliable and accurate results than the usual method of numerical central differential, as reported by Matlock (1958) and Yang and Liang (2006). The method was used to calculate the soil reaction by assuming zero moment and shear force at the pile-tip (which has limited impact on the results, Guo and Lee, 2001). It is written into a spreadsheet program via Microsoft Excel VBA. For each measured frame movement, the program offers five profiles of bending moment, shear force, soil reaction, rotation and deflection, the maximum bending moment M_{max}, maximum shear force T_{max}, and pile deflection at the model ground surface y_0. Typical measured data calculated from this program are discussed next

3.1 Response of pile during test TS32-588

Test TS32-588 was conducted at an axial load of 588 N, a sliding layer depth L_m = 200 mm, and a stable layer L_s = 500 mm. Figs. 4(a) through (e) show the bending moment, shear force, soil reaction, pile rotation and deflection profiles at each 10 mm of frame movement until w_f = 120 mm.

The bending moment profiles (see Fig. 4(a)) are analogous to a parabolic shape at w_f $\geq$ 40 mm. The maximum moment M_{max} occurs at a depth of 400 mm down the pile below the ground surface. Two large shear forces were noted at depths of 250 mm and 550 mm in Fig. 4(b), respectively. The free-headed pile deflection is mainly caused by rotation around pile tip in Fig. 4(c). As expected, the soil movement results in positive soil pressure on the pile above the sliding depth in Fig. 4(e), and active resistance in the middle part of the pile (from depth 200 mm to the reverse point at 550 mm). It must be stressed that the deflection y is generally equal to the relative pile-soil displacement for the current tests, otherwise it should be reduced by the amount of the translating deformation (pile and soil moving together) as discussed elsewhere. The reverse direction of on-pile force per unit length p in Fig. 4(c), is associated with that change of gradients of the rotation seen in Fig. 4(b).

Fig. 4 shows that response of the pile is negligible at a frame (thus soil) movement of $w_f \leq 40$ mm; afterwards, it increases rapidly with the movement w_f, and reaches the peak values at $w_f = 70$ mm. For example, the M_{max} rises sharply from 19.2 kNmm ($w_f = 40$ mm) to 89.7 kNmm ($w_f = 70$ mm). Finally ($w_f > 70$ mm), it decreases slightly and remains more or less constant. At $w_f = 120$ mm, the pile deflection y_0 is 15.8 mm, which is only 13.2% of the frame movement. The sand at the ground surface had flowed around the pile during the test.

3.2 Response of M_{max}, T_{max} and y_0 versus w_f

Figs. 5(a,b,c) through 8(a,b,c) show the measured maximum bending moment M_{max}, the deduced maximum shear force T_{max}, and pile deflection at ground surface y_0 with frame movement w_f for the four series of tests. The associated values at typical frame movements are provided in Table 2. All piles have similar response of M_{max}, T_{max}, and y_0 versus w_f to that of the standard test TS32-0, but for the following differences:

(1) In series 1 and 2, the piles have a trivial response at $w_f < 40$ mm; a sharp increase in M_{max} (T_{max}) with 40 mm $\leq w_f <$ 70~80 mm, and a near constant (with some softening) critical response afterwards. Interestingly, the y_0 versus w_f curves remain stable.

(2) In series 3, the frame movement causes little pile response until w_f exceeds 60 mm and 80 mm for TS32-0 (22.5°) and TS32-0 (30°); and the critical responses peaked at $w_f = 100$ mm and 120 mm, respectively.

(3) In series 4, the frame movement causes very little reaction on the tested pile in T32-0 (L_m=125) even at $w_f = 150$ mm. The pile response of TS32-0(L_m= 250) peaked at $w_f = 120$ mm. In contrast, the critical pile response in tests T32-0 (L_m=300) and T32-0 (L_m=350) have not reached the peak values even at a frame movement w_f of

150 mm.

3.3 Typical bending moment, shear force and deflection profiles

Figs. 5(d,e,f,) through 8(d,e,f) show the measured maximum bending moment profiles, deduced shear force and pile deflection profiles at the larger frame movement w_f given in Table 2. These figures demonstrate that

(1) The distribution of bending moment along the pile is of a parabolic shape.

(2) The maximum bending moment M_{max} occurs at a depth of 370 ~ 475 mm in the stable layer, with an average at 410 mm (≈ 3/5 the pile embedment length).

(3) The shear force profiles are of a similar shape, and with similar maximum magnitudes in the stable layer (positive) and in the sliding layer (negative).

(4) Pile deflected mainly by rotation around pile tip.

4. Discussion

4.1 Effect of distance between pile and soil movement source

The effect of the distance between soil movement source and the pile was investigated by installing the pile at a distance S_b of 340 mm (TS32-0-340), 500 mm (TS32-0) and 660 mm (TS32-0-660) (note L_m = 200 mm). The measured pile responses are shown in Fig. 5, which indicate similar variation laws to those of the standard test TS32-0, as described previously and by Guo and Qin (2010). However, the gradient of the linear increase in the M_{max} with the w_f (40~80 mm) decreased with the increasing distance S_b. As plotted in Fig. 9(a), the M_{max} reduced by~ 32 kNmm as the pile was relocated from S_b = 340 mm to 500 mm, and reduced further by ~ 10 kNmm from S_b= 500 mm to 600 mm. The initial frame movements, w_i (for negligible pile responses) are plotted in Fig. 9(b) against the distance S_b. It has little variation with the pile location.

Fig. 10 shows the soil movement around the pile at the ground surface at w_f = 20, 60, 100 and 130 mm. Wedges characterized by ‘sand heaves’ were observed on the ground surface with the furthest one measured ~ 330 mm from the loading block side at w_f = 130 mm (see Fig. 10(d)). The wedge was originally located at a distance of

460 mm (=330+130, mm) from the loading side. Similar sand upward heaves at the ground surface were observed by Suleiman et al. (2014) in their experiment. The soil movement field at the ground surface indicates sand flowed around parts of the pile within the failure zone, and remained intact outside the failure zone (see Figs. 10(c) and (d)). The upward passive heave failures and failure wedge at the displacement boundaries do not support the numerical assumption of sliding layer moving as a rigid body over the stable layer by Kourkoulis et al. (2011) and the soil movements acting on the pile are not the same as the frame movement.

The piles in test TS32-0-340 and TS32-0-660 were 340 mm, and 660 mm, respectively, away from the loading block side. They are within and outside the failure zone even at a large frame movement of 130 mm. The attenuation (thus non-uniform mobilization) of soil movement from the loading side to the pile location reduces the maximum bending moment.

4.2 Effect of magnitude of axial load

The effect of axial load on the pile response was examined by varying the axial load at head from 0 N to 735 N. Along with TS32-0 and TS32-294 tests presented by Guo and Qin (2010), two additional tests TS32-588 and TS32-735 were conducted at an axial load of 588 N and 735 N, respectively. The measured response is presented in Fig. 6. The axial load causes a small (< 20% of M_{max}) bending moment at the ground surface; otherwise it has limited impact on the bending moment and shear force profiles and the evolvement pattern of M_{max} and T_{max} with frame movement w_f. The pile rotated about the pile-tip in TS32-0 and TS32-294, and about a depth of 500 mm (about 0.7*L*) in TS32-735. The latter pile-tip 'kicked out' about 3.8 mm in the opposite direction. The axial load generally increases the pile responses. For instance, an increase in the axial load from 0 N to 735 N on the pile head leads to: (1) an 80% increase in M_{max}; and (2) an 80% and 37% increase in T_{max} in the stable layer and sliding layer, respectively.

4.3 Effect of loading block angle

In order to examine the pile response to direction of soil movement (via block angle θ), another two loading blocks were made to an angle of 22.5° and 30° as shown in Fig. 2. Tests TS32-0 (22.5°) and TS32-0 (30°) were conducted using block 2 (θ = 22.5°) and block 3 (θ = 30°), respectively, under the same conditions as the 'standard' test TS32-0. The results are presented in Fig. 7, which indicate similar characteristics among the three tests, but for increase in the initial frame movement w_i from 50 mm in TS32-0 (22.5°) to 80 mm in TS32-0 (30°), which are 1.35 and 2.16 times the 37 mm in the standard test TS32-0.

The tests are analogous to simple shear tests until the predetermined sliding depth is attained, for instance, at $w_f \leq 70$ mm for TS32-0. Thereafter, the frames above a selected sliding surface were translated together. The sequential frame movements in lateral and vertical dimensions using the three loading blocks are provided in Table 3. They are plotted in Fig. 11(a). The loading block 1 (θ =15°), block 2 (θ =22.5°), or block 3 (θ =30°) mobilize the predetermined final depth L_m = 200 mm at a frame movement w_f of 60 mm (TS32-0 (15°)), 90 mm (TS32-0 (22.5°)), and 110 mm (TS32-0 (30°)), respectively. At an extreme θ = 0°, the triangular loading block degrades to a rectangular one, and generates a uniform translational frame movement as discussed by Qin and Guo (2010a). The peak M_{max} and the initial frame movement w_i are plotted in Fig. 11(b) against the loading block angle θ. The M_{max} for θ = 0° was obtained from test RS32-0 reported by Guo and Ghee (2005). The peak M_{max} and the w_i are linearly related to the loading block angle θ

$$M_{max} = 1.4*\theta+25 \quad (1)$$

$$w_i = 2.8*\theta \quad (2)$$

where M_{max} is peak maximum bending moment (kNmm), and θ is loading block angle (degree). The moment M_{max} and angle θ are also shown in Fig. 12 (right) for the moment of reaching sliding depth (w_a), and at the frame movement w_p, respectively.

Cai and Ugai (2003) studied the response of flexible piles under an inverse triangular distribution of soil movement (with zero movement at the sliding depth).

They demonstrated that increasing the inclination, θ_0 between the pile axis and the soil movement profile leads to higher maximum bending moment in the stable layer. Their angle θ_0, however, essentially refers to the inclination of the soil movement profile at the pile location, rather than the loading block angle.

The current tests were conducted by using a triangular block with a fixed angle θ, and a constant pile embedment depth. Chen (1994) conducted similar laboratory tests by applying an inverse triangular profile of lateral soil movement at the loading location through rotating a steel plate about a fixed sliding depth in a container (see the inset in Fig. 12). They varied the sliding depth L_m (thus pile embedment depth, L) between 200 mm and 350 mm and used a fixed stable layer depth L_s (= 325 mm). Chen's test results were re-interpreted here in terms of the apparatus wall rotational angle θ about its toe. The angle was calculated as the ratio of the soil surface movement w_f over the sliding layer depth L_m. The measured peak values of $M_{\max}$ are plotted in Fig. 12 against the wall rotation together with the current tests (for loading block angle θ). The figure indicates a fast increase in the maximum bending moment M_{max} at a low rotation angle $\theta < 12^{o}$. At a specific rotation angle θ, increasing in sliding layer depth, L_m (L_s = constant) results in larger maximum bending moment M_{max}. For instance, at $\theta = 5°$ and $L_s = 325$ mm, M_{max} increases from 3.63 to 28.8 kNmm as L_m increases from 200 to 350 mm.

4.4 Effect of sliding layer depths

The effect of varying sliding layer depth on the pile responses was investigated by conducting five tests at a predetermined final sliding depth of L_m=125, 200, 250, 300 and 350 mm (a constant pile embedment of 700 mm), respectively. The test results are plotted in Fig. 8. The triangular loading block not only causes horizontal frame movement but also gradually mobilizes the deeper frames. This results in a progressively moving soil profile at the loading side. To quantify the impact of depth of moving soil layer, a sliding depth ratio R_L (= L_m/L) was introduced by Guo and Qin (2010) as the ratio of thickness of moving soil L_m over the pile embedment length L.

Table 3 presents the progressively moving sand depth L_m, with frame movement w_f, and the calculated sliding depth ratio R_L. The predetermined final sliding depths of 125, 200, 250, 300, and 350 mm correspond to final sliding depth ratios of 0.179, 0.286, 0.357, 0.429 and 0.5, respectively. Fig. 13 shows the variation of the maximum bending moment M_{max} (or maximum shear force $T_{max} = M_{max}/0.357L$) with the sliding depth ratio R_L, which is characterized by

(1) a negligible M_{max} (or T_{max}) in the pile at R_L<0.17 (w_f<37 mm);

(2) increasing M_{max} with increasing R_L until a final sliding depth ratio R_L of 0.179, 0.286, 0.357, 0.429 and 0.5 was just attained, respectively; and

(3) an augment of M_{max} (or $T_{\max}$) at the final constant R_L caused by the trapezoidal frame movement. The magnitudes of M_{max} are 5.2, 62.6, 115.3, and 118.1 kNmm upon reaching the pre-determined L_m; and increased finally to 5.7, 123.5, 175.0, and 140.0 (not yet to limit) kNmm, respectively.

The increase in M_{max} with increase in sliding depth ratio R_L in the tested range of R_L= 0~0.5 is consistent with the findings from similar model tests reported by Chen (1994) and Poulos et al. (1995). Importantly, the current tests reveal additional increase in the M_{max} at the final R_L due to the translation of the frames (trapezoidal movement), as explained previously (see inset in Fig. 12).

The effect of sliding depth relative to pile embedded length has also been investigated through analytical and numerical analysis in undrained and drained conditions (Vigianni, 1981, Poulos, 1995, Kanagasbai et al., 2011, Kourkoulis et al., 2011, Muraro et al., 2014, Suleiman et al., 2007, Guo, 2014a). Three pile-soil interaction modes have been identified: flow mode, intermediate mode and short mode. All the five tests in series 4 show the "flow mode" behavior even for test T32-0 (L_m=350) at R_L = 0.5, including a more or less parabolic distributed bending moment profile with maximum bending moment developed in the stable layer (Fig. 8(a)), and displacement due to rigid rotation (Fig. 8(c)). The flow mode of the current tests is associated with L_s/L_m = 1 ~ 4.6, which agree with $L_s/L_m \geq 1.2$ obtained using the limit equilibrium analysis by Muraro et al. (2014) for a rigid passive pile in drained condition.

4.5 Experimental relationship between M_{max} and T_{max}

Figs. 14(a) and 14(b) plot the maximum shear force in both the sliding (T_{max2}) and stable (T_{max}) layers, respectively, against the maximum bending moment M_{max} for a frame movement up to w_i and the extra-large w_f for the trapezoidal movement. Linear relationships (to an accuracy of ~8%) were observed between M_{max} and T_{max}

$M_{max}=T_{\max}L/2.8$ or $M_{max}=T_{max2}L/2.6$ (3)

The correlations are identical to those established previously (Guo and Qin, 2010). They are thus independent of the loading angle (direction of soil movement).

5. Estimation of M_{max} and T_{max} with w_f

5.1 Simple elastic solution

Guo and Qin (2010) assume the maximum shear force T_{max} (induced in piles subjected to lateral soil movement) as an equivalent lateral load on an active pile, and proposed the following elastic solution to estimate the force T_{max} and the moment M_{max}

$$T_{\max}=(w_{\mathrm{f}}-w_{\mathrm{i}})kL/4 \quad (4)$$

$$M_{\max}=\mathrm{m}(w_{\mathrm{f}}-w_{\mathrm{i}})kL^2/4 \quad (5)$$

where L is the pile embedment; k is the subgrade reaction modulus; w_f is the frame movement; w_i is an initial frame movement that causes negligible pile response, and m (= 0.357 ~ 0.385 as deduced from Eq. (3)) is a non-dimensional constant. The solution offers satisfactory predictions of the pile responses under four testing conditions (Guo and Qin 2010): (1) the standard TS and TD series tests (2) different sliding depths (constant L); (3) varying position of soil movement; and (4) varying sliding depths (any L). Guo (2012) indicates T_{max} = $0.5A_{\mathrm{L}}dL_{\mathrm{m}}^2$, in light of a linearly increasing of force per unit length (p_{u}) with depth (z): p_{u} = $A_{\mathrm{L}}dz$, in which A_{L} = $(0.4\sim1.0)\gamma_{\mathrm{s}}'K_{\mathrm{p}}^2$; $K_{\mathrm{p}}= \tan^2(45^{\mathrm{o}}+\phi'/2)$, coefficient of passive earth pressure; ϕ' = an effective frictional angle of soil; γ_{s}' = an effective unit weight of the soil (dry weight above the water table, buoyant weight below). The p_{u} alters with soil movement profiles, although it is generally independent of pile properties under lateral loading.

5.2. Calculation of M_{max} and T_{max} with frame movement

Eqs. (4) and (5) are used for evaluating the current test results. The three parameters w_i, m, and k are determined using the test data and shown in Table 2.

● The initial frame movement w_i is estimated as 37 mm for test T32-0 (L_m=300), and 89 mm for test TS32-0 (30°), as is seen from the measured $M_{max} \sim w_f$ curves.

● m = 0.357 is obtained from the linear relationship between M_{max} and T_{max} in Fig. 14.

● k (= (2.4~3)G_s) and G_s were deduced from the overall shear process of the pile-soil-shear box system (Guo and Qin 2010)

The predicted M_{max} and T_{max} with the evolvement of w_f were plotted as solid lines in Figs. 5 (a,b) through 8(a,b) using the parameters k and w_i. The figures show:

- The subgrade modulus k reduces by 54% as the distance S_b increases from 340 mm to 660 mm, as shown in Fig. 9(b).
- The loading block angle only affects the initial frame movement, w_i but not the subgrade modulus k.
- Using the loading block 1 (θ =15°), the variation of sliding depth ratio R_L (from 0.179 to 0.50) does not significantly affect the initial frame movement w_i. The deduced k falls in a range of 38 ~ 45 kPa, and is within ± 10% of the 42 kPa obtained in the standard test TS32-0.
- The increase of subgrade modulus in test TS32-588 and TS32-735 is attributed to the p ~ Δ effect, as additional bending moment is generated by the axial load.

As noted before (Guo and Qin, 2010), Eqs. (4) and (5) offer continuous increase values of pile moment M_{max} (thus shear force T_{max}), which should be capped by, e.g. the M_{max} envelope in Fig. 13.

5.3 Validation against boundary element analysis and an in-situ pile

Eqs (4) and (5) were compared with the boundary element analysis (via the program PALLS) by Chen and Poulos (1997) on an unrestrained free-head model pile. The pile is embedded to a depth of 675 mm with a sliding layer, L_m of 350 mm and a stable layer, L_s of 325 mm, respectively (Poulos et al. 1995). The calculated maximum bending moment from full analysis by PALLS compared well with the measured values for the measured soil surface movement (see Fig 15(a)), despite a substantial overestimation of the moment using their elastic design chart solutions.

Qin (2010) re-evaluated the test results. The bending moment profiles were fitted using 5th order polynomial functions, from which the shear force profiles were derived. A ratio m=$M_{\max}/T_{\max}L$ of 0.30 was determined as shown in Fig. 15(b). The $M_{\max}$ is calculated using $M_{\max}= w_f kL^2/13.33$ with w_i = 0 (as observed), L= 0.675 m, and k = 16.2 kPa (Guo and Qin, 2010), which gives $M_{\max}= 0.55w_f$ (kNmm, w_f in mm). This calculated M_{max} is plotted against the soil surface movement in Fig 15(c) with the measured data. It is less than the measured M_{max}. An accurate estimation requires a modulus k of 24 kPa.

Lirer (2012) reported a field trial test on a row of five piles installed into an active mudslide (with a sliding depth of 5 m) in highly fissured plastic clay. The piles were 10 m long, 0.4 m in diameter, and installed at a spacing of 0.9 m. They had an ultimate bending moment of 250 kNm. An inclinometer tube was installed on the uphill side of the middle pile to measure the pile displacement. Another two inclinometers were placed uphill and downhill, and 1.5 m away from the pile. The measurements were recorded over 3 years. The measured pile displacement increases approximately linearly from ground surface to a depth of 6 m, at which the pile formed a plastic hinge. The bending moment and shear force profiles were obtained from successive derivations of a ninth-order polynomial curve fitting of the measured pile displacement profile.

The pile exhibits B2 failure mode (Viggiani, 1981) or the intermediate mode with pile failure (Poulos 1995) at a sliding depth ratio R_L = 0.5, in which a peak bending moment developed in the sliding and stable layer, respectively; and the maximum shearing force T_{max} occurred at the sliding depth (z = 5 m). Fig. 16(a) plots the maximum shear force T_{max} against the absolute maximum bending moment M_{max} at the depth of 6 m in the stable layer. A linear relationship is evident between the T_{max}

and M_{max} (independent of ground movement), and m=$M_{max}/T_{max}L$= 0.333 (L = 6.0 m). Fig. 16(b) shows the development of maximum shear force T_{max} with the ground displacement measured at the head of the uphill inclinometer. The T_{max} is calculated using $T_{max}= w_f kL/4$, $w_i = 0$, L= 6.0 m, and k = 500 kPa (=10S_u, where undrained shear strength S_u = 50 kPa). The calculated T_{max} values agree well with the measured data up to the failure load of 100 kN at which a plastic hinge was developed in the pile.

6. Concluding remarks

With an experimental apparatus developed, the behavior of vertically loaded, free head piles subjected to progressive soil movement was investigated by conducting ten new model tests on instrumented single piles in dry sand. The induced bending moment, shear force and deflection along the piles were presented. The development of maximum bending moment, maximum shear force and pile deflection at the ground surface with soil movement were provided as well. The effects of axial load, distance between pile and source of free soil movement, sliding depths, and loading block angle were assessed. The current test results further corroborate the previous findings such as the linear relationship between M_{max} and T_{max} by Guo and Qin (2010). The main conclusions are as follows

- The M_{max} is linearly related to the T_{max} by $M_{max} = T_{max}L/(2.6 \sim 2.8)$, irrespective of the pile location, axial load level, sliding depth ratio and loading block angle.
- Increasing distance S_b reduces the M_{max}, T_{max} and pile displacement at ground surface y_0. Axial load causes additional bending moment and deflection in free-head, passive piles.
- The pile bending moments and deflections were negligible for a sliding depth ratio R_L < 0.17; and increase 'linearly' with R_L afterwards until the cap values. The M_{max} increases by 10% ~ 97% (with an average of 48%) at the final sliding depth due to the trapezoidal (translational) movement of the frames induced by the triangular loading block.
- The M_{max} and w_i increase linearly with the loading block angle θ, which observe

M_{max} =1.4*θ + 25 and w_i =2.8*θ (θ in degrees) for the present model tests.

- The elastic solution of Eqs. (4) and (5) offers satisfactory prediction of the development of M_{max} and T_{max} with soil movement for the 13 model test piles and an in situ test pile, as with previous study.

Acknowledgements

The work reported herein was supported by an Australian Research Council Discovery Grant (DP0209027). The financial assistance is gratefully acknowledged.

References

Ashour, M., and Ardalan, H., 2012, “Analysis of pile stabilized slopes based on soil-pile interaction,” *Comput. Geotech.,* Vol. 39, pp. 85-97.

Brandenberg, S. C., Boulanger, R.W., and Kutter, B. L., 2005, “Discussion of ‘Single piles in lateral spreads: field bending moment evaluation’,” *J. Geotech. Geoenviron. Eng.,* Vol. 131, No. 4, pp. 529-531.

Bransby, M. F., and Springman, S.M., 1997, “Centrifuge modeling of pile groups adjacent to surcharge loads,” *Soils Found.*, Vol. 37, No. 2, pp. 39-49.

Byrne, B.W., 2014, “Laboratory scale modelling for offshore geotechnical problems,” *Physical Modelling in Geotechnics*, C. Gaudin, and D. White, Eds, Taylor & Francis Group, London, pp. 61-75.

Byrne, P. M., Anderson, D. L., and Janzen, W., 1984, “Response of piles and casings to horizontal free-field soil displacements,” *Can. Geotech. J.*, Vol. 21, No.4, pp. 720-725.

Cai. F., and Ugai, K., 2000, “Numerical analyses of the stability of a slope reinforced with piles,” *Soils Found.*, Vol. 40, No. 1, pp. 73-84.

Cai. F. and Ugai, K., 2003, “Response of flexible piles under laterally linear movement of the sliding layer in landslides,” *Can. Geotech. J.*, Vol. 40, No. 1, pp. 46-53.

Cai. F. and Ugai, K., 2011, “A subgrade reaction solution for piles to stablise landslides,” *Geotechnique,* Vol. 61, No. 2, pp. 143-151.

Chen, C.Y., and Martin, G. R., 2002, “Soil-structure interaction for landslide stabilizing piles,” *Comput. Geotech.,* Vol. 29, pp. 363-386.

Chen, L. T., 1994, “The effect of lateral soil movements on pile foundations,” Ph.D. thesis, University of Sydney, Sydney, Australia.

Chen, L. T., and Poulos, H.G., 1997, “Piles subjected to lateral soil movements,” *J. Geotech. Geoenviron. Eng.,* Vol. 123, No. 9, pp. 802-811.

Chen, L. T., Poulos, H.G., and Hull, T.S., 1997, “Model tests on pile groups subjected to lateral soil movement,” *Soils Found.,* Vol. 37, No. 1, pp. 1-12.

Chmoulian, A. Y., 2004, "Briefing: analysis of piled stabilization of landslides," *Proc. Inst. Civ. Eng. Geotech. Eng.,* Vol. 157, No. 2, pp. 55-56.

Chow, Y. K., 1996, "Analysis of piles used for slope stabilization," *Int. J. Numer. Anal. Methods in Geomechanics,* Vol. 20, No. 9, pp. 635-646.

De Beer, E. E., 1977, "Piles subjected to static lateral loads," *Proceedings of 9th International Conference on Soil Mechanics and Foundation Engineering*, Specialty Session No. 10, Tokyo, 1-14.

Dobry, R., Abdoun, T., O'Rourke, T. D., and Goh, S. H., 2003, "Single piles in lateral spreads: field bending moment evaluation," *J. Geotech. Geoenviron. Eng.,* Vol. 129, No. 10, pp. 879-889.

Ellis, E.A., and Springman, F. M., 2001, "Full-height piled bridge abutments constructed on soft clay," *Geotechnique,* Vol. 51, No. 1, pp. 3-14.

Ellis, E.A., Durrani, I. K., and Reddish, D. J., 2010, "Numerical modelling of discrete pile rows for slope stability and generic guidance for design," *Geotechnique*, Vol. 60, No. 3, pp. 185-195.

Fioravante, V., 2008, "Physical modeling of landslide stabilization methods in an overconsolidated clay," *Geotech. Test. J.*, Vol. 31, No. 2, pp. 1-17.

Frank, R., and Pouget, P., 2008, "Experimental pile subjected to long duration thrusts owing to a moving slope," *Geotechnique,* Vol. 58, No. 8, pp. 645-658.

Fukuoka, M., 1977, "The effects of horizontal loads on piles due to landslides," *Proc. 9th International Conference on Soil Mechanics and Foundation Engineering*, Specialty Session 10, Tokyo, 77-80.

Galli, A. and di Prisco, C., 2013, "Displacement-based design procedure for slope stabilizing piles," *Can. Geotech. J.*, Vol. 50, No. 1, pp. 41-53.

Ghee, E. H., 2010, "The response of axially loaded piles subjected to lateral soil movements," Ph.D. Thesis, Griffith University, Gold Coast, Australia.

Guo, W. D., 2013, "P_u-based solutions for slope stabilizing piles," *Int. J. Geomech.,* Vol. 13, No. 3, pp. 292-310.

Guo, W. D., 2012, *Theory and practice of pile foundations*. Boca Raton, London, New York, CRC

Guo, W. D., 2014a, “Elastic models for nonlinear response of rigid passive piles,” *Int. J. Numer. Anal. Methods in Geomechanics,* Vol. 38, No. 18, pp. 1969-1989.

Guo, W. D., 2014b, “Nonlinear response of laterally loaded rigid piles in sliding soil,” *Can. Geotech. J.,* in press

Guo, W. D., Ghee, E. H., 2004, “Model tests on single piles in sand subjected to lateral soil movement,” *Proc. of the 18th Australasian Conference on the Mechanics of Structures and Materials*, A. Deeks and H. Hao, Eds., Taylor & Francis Group, London, Vol. 2, pp. 997-1003.

Guo, W. D., and Ghee, E. H., 2005, “A preliminary investigation into the effect of axial load on piles subjected to lateral soil movement,” *Frontiers in Offshore Geotechnics,* ISFOG2005, S. Gourvence, and M. Cassidy, Eds., Taylor & Francis Group, London, pp. 865-871.

Guo, W. D. and Lee, F. H. (2001), "Load transfer approach for laterally loaded piles." *International Journal of Numerical & Analytical Methods in Geomechanics*, **25**(11): 1101-1129.

Guo, W. D., and Qin, H. Y., 2005, “Vertically loaded single piles in sand subjected to lateral soil movements,” *Proc. 6th Inter. Conf. on Tall Building*, Hong Kong, pp. 327-332.

Guo, W. D., Qin, H. Y., 2006, “Vertically loaded piles in sand subjected to triangular profiles of soil movements,” *Proc. 10th Inter. Conf. on Piling and Deep Foundations*, Amsterdam, pp. 296-302.

Guo, W. D., Qin, H. Y., and Ghee, E. H., 2006, “Effect of soil movement profiles on vertically loaded single piles,” *Physical Modelling in Geotechnics,*, C. W. W. Ng., L. Zhang, and Y. Wang, Eds., Taylor & Francis Group, London, Vol. 2, pp. 841-846.

Guo, W. D., Qin, H. Y., 2010, “Thrust and bending moment of rigid piles subjected to moving soil,” *Can. Geotech. J.*, Vol. 47, No. 2, pp. 180-196.

Ito, T. and Matsui, T., 1975, “Methods to estimate lateral force acting on stabilizing piles,” *Soils Found.*, Vol. 15, No. 4, pp. 43-59.

Kanagasabai, S., Smethurst, J. A., and Powrie, W., 2011, “Three-dimensional numerical modeling of discrete piles used to stabilize landslides,” *Can. Geotech. J.*, Vol. 48, No. 11, pp. 1393-1411.

Katzenbach, R., Bachmann, G., and Gutberlet, C., 2005, "Pile-soil-wall interaction during the construction process of deep excavation pits," *Proceedings of Sixteenth International Conference on Soil Mechanics and Geotechnical Enigneering*, Osaka, pp. 1501-1504.

Kourkoulis, R., Gelagoti, F., Anastasopoulos, I., and Gazatas, G., 2011, "Slope stabilizing piles and pile-groups: parametric study and design insights," *J. Geotech. Geoenviron. Eng.,* Vol. 137, No. 7, pp. 663-677.

Kourkoulis, R., Gelagoti, F., Anastasopoulos, I., and Gazatas, G., 2012, "Hybrid method for analysis and design of slope stabilizing piles," *J. Geotech. Geoenviron. Eng.,* Vol. 138, No. 1, pp. 1-14.

Leung, C.F., Chow, Y. K., and Shen, R.F., 2000, "Behavior of pile subject to excavation-induced soil movement," *J. Geotech. Geoenviron. Eng.,* Vol. 126, No. 11, pp. 947-954.

Leung, C.F., Lim, J.K., Shen, R.F., and Chow, Y. K., 2003, "Behavior of pile groups subject to excavation-induced soil movement," *J. Geotech. Geoenviron. Eng.,* Vol. 129, No. 1, pp. 58-65.

Leung, C.F., Ong, D.E.L., and Chow, Y. K., 2006, "Pile behavior due to excavation-induced soil movement in clay. Π: collapse wall," *J. Geotech. Geoenviron. Eng.,* Vol. 132, No. 1, pp. 45-53.

Levachev, S. N., Fedorovsky, V.G., Kurillo, S.V., and Kolesnikov, Y. M., 2002, *Piles in hydrotechnical engineering*, Taylor and Francis, London.

Liang, R. Y., and Yamin, M., 2009, "Three dimensional finite element study of arching behavior in slope/drilled shafts system," *Int. J. Numer. Anal. Methods in Geomechanics,* Vol. 34, No. 11, pp. 1157-1168.

Lirer, S., 2012, "Landslide stabilizing piles: experimental evidences and numerical interpretation," *Eng. Geol.*, Vol. 149, No. 4, pp. 70-77.

Matlock, H. M., 1958, "Discussion on 'Soil modulus for laterally loaded piles'. *Transactions, ASCE*, Vol. 123, pp. 1077-1081.

Muraro, S., Madaschi, A. and Gajo, A., 2014, "On the reliability of 3D numerical analyses on passive piles used for slope stablisation in frictional soils," *Geotechnique*, Vol. 64, No. 6, pp. 486-492.

O'Kelly, B. C., Ward, P. N., and Raybould, M. J., 2008, "Stabilization of a progressive railway embankment slip," *Geomech. Geoengineering: An Int. J.*, Vol. 3, No. 4, pp. 231-244.

Ong, D.E.L., Leung, C.F., and Chow, Y. K., 2006, "Pile behavior due to excavation-induced soil movement in clay. I: stable wall," *J. Geotech. Geoenviron. Eng.,* Vol. 132, No. 1, pp. 36-44.

Ong, D.E.L., Leung, C.F., and Chow, Y. K., 2009, "Behavior of pile groups subjected to excavation-induced soil movement in very soft clay," *J. Geotech. Geoenviron. Eng.,* Vol. 135, No. 10, pp. 1462-1474.

Pan, D., Smethurst, J. A., and Powrie, W., 2012, "Limiting pressure on a laterally loaded pile in a frictional soil," *Geotechnique Letter,* Vol. 2, 55-60.

Pan, J. L., Goh, A.T.C., Wong, K.S., and Teh, C. I., 2000, "Model tests on single piles in soft clay," *Can. Geotech. J.*, Vol. 37, No. 4, pp. 890-897.

Pan, J. L., Goh, A.T.C., Wong, K.S., and Teh, C. I., 2002, "Ultimate soil pressures for piles subjected to lateral soil movements," *J. Geotech. Geoenviron. Eng.,* Vol. 128, No. 6, pp. 530-535.

Poulos, H. G., 1973, "Analysis of piles in soil undergoing lateral movement," *J. Soil Mech. Found. Eng.*, Vol. 99, No. 5, pp. 391-406.

Poulos, H. G., 1995, "Design of reinforcing piles to increase slope stability," *Can. Geotech. J.*, Vol. 32, No. 5, pp. 808-818.

Poulos, H.G., Chen, L. T., and Hull, T.S., 1995, "Model tests on single piles subjected to lateral soil movement," *Soils Found.,* Vol. 35, No. 4, pp. 85-92.

Qin, H. Y., 2010, "Response of pile foundations due to lateral force and soil movements," Ph.D. thesis, Griffith University, Gold Coast, Australia.

Qin, H. Y., and Guo, W. D., 2010a, "Pile response due to lateral soil movement of uniform and triangular profiles," *GeoFlorida2010: Advances in analysis, modelling and design*, D. Fratta, A. Puppala, and B. Muhunthan, Geotechnical Special Publications (GSP) GSP 199, pp. 1515-1522.

Qin, H. Y., and Guo, W. D., 2010b, "Pile response subjected to effective soil movement," *Physical Modelling in Geomechanics*, S. Springman, J. Laue, and L. Seward, Eds., Taylor and Francis, London, pp. 823-828.

Randolph, M. F., and House, A. R., 2001, "The complementary roles of physical and computational modelling," *Int. J. Physical Model. Geotech.*, Vol. 1, No. 1, pp. 1-8.

Reese L. C., Wang, S. T., and Fouse, J. L., 1992, "Use of drilled shafts in stabilizing a slope," *Stability and performance of slopes and embankments*. R. Seed, and R. Boulanger, Eds., ASCE, Vol. 2, pp. 1318-1332.

Smethurst, J. A., and Powrie, W., 2007, "Monitoring and analysis of the bending behaviour of discrete piles used to stabilize a railway embankment," *Geotechnique*, Vol. 57, No. 8, pp. 663-677.

Stewart, D. P., Jewell, R. J., and Randolph, M. F., 1994, "Design of piled bridge abutment on soft clay for loading from lateral soil movements," *Geotechnique*, Vol. 44, No. 2, pp. 277-296.

Suleiman, M. T., Ni, L., Helm, J. D., and Raich, A., 2014, "Soil-pile interaction for a small diameter pile embedded in granular soil subjected to passive loading," *J. Geotech. Geoenviron. Eng.,* Vol. 140, No. 5, pp. 04014002-1 -15.

Suleiman, M. T., Schaefer, V. R., and Ho, I. H. 2007. "Behavior of piles used for slope remediation," *1st North American Landslide Conference*. Landslides and Society: Integrated Science, Engineering, Management, and Mitigation (CD-ROM), Association of Environmental and Engineering Geologists, Denver.

Viggiani, C., 1981, "Ultimate lateral load on piles used to stabilize landslides," *Proceedings of 10th International Conference on Soil Mechanics and Foundation Engineering*, Stockholm, Vol.3, pp. 550-560.

White, D. J., Thompson, M. J., Suleiman, M. T., and Schaefer, V. R., 2008, "Behavior of slender piles subject to free-field lateral soil movement," *J. Geotech. Geoenviron. Eng.,* Vol. 134, No. 4, pp. 428-436.

Yang, K., and Liang, R., 2006, "Methods for deriving p-y curves from instrumented lateral load tests," *Geotech. Test. J.*, Vol. 30, No. 1, pp. 1-8.

Yap, T. Y. and Pound C., 2003, "A numerical study of the influence of piles in the passive zone of embedded retaining walls," *FLAC and Numerical modeling in Geomechanics*, Proceedings of the 3rd International FLAC Symposium, Sudbury, Canada, Taylor and Francis, pp. 301-309.

Yoon, B. S., and Ellis, E. A., 2009, "Centrifuge modelling of slope stabilization using a discrete pile row," *Geomech. Geoeng.: An Int. J.*, Vol. 4, No. 2, pp. 103-108.

Table 1 Details of the model tests

Test number	Test description	Outer Diameter D (mm)	Axial load P (N)	Sliding layer depth L_m (mm)	Stable layer depth L_s (mm)	Sliding Depth Ratio R_L (L_m/L)	Test series
1	TS32-0†	32	0	200	500	0.286	Standard test
11	TS32-0-340*	32	0	200	500	0.286	Series 1 Pile location, S_b
12	TS32-0-660*	32	0	200	500	0.286	
13	TS32-294†	32	294	200	500	0.286	Series 2 Axial load, P
14	TS32-588	32	588	200	500	0.286	
15	TS32-735	32	735	200	500	0.286	
16	TS32-0 (θ=22.5°)‡	32	0	200	500	0.286	Series 3 Loading block angle, θ
17	TS32-0 (θ=30°)‡	32	0	200	500	0.286	
18	T32-0 (L_m=125)	32	0	125	575	0.179	Series 4 Sliding depth, L_m
19	T32-0 (L_m=250)	32	0	250	450	0.357	
20	T32-0 (L_m=300)	32	0	300	400	0.429	
21	T32-0 (L_m=350)	32	0	350	350	0.5	

* Pile location, S_b=340, 660mm ‡ Loading block angle θ=22.5°, 30° † Reported previously by Guo and Qin (2010)

Test description	Frame movement w_f (mm)	Maximum Bending moment M_{max} (kNmm)	Depth of M_{max} z_{max} (mm)	Maximum Shear force T_{max} (N)		Deflection at ground surface y_0 (mm)	Initial frame Mvt w_i (mm)	Subgrade modulus k (kPa)
				Stable layer	Sliding layer			
TS32-0†	<u>60</u> 70	<u>39.3</u> 49.7	370	<u>147.2</u> 183.8	<u>159.8</u> 201.1	<u>7.1</u> 10.3	40	42

Table 2 Summary of test results

TS32-0-340	60 80	63.8 81.0	400	266.9 327.7	266.6 325.8	11.5 14.8	37	65
TS32-0-660	60 80	30.0 40.0	400	114.9 150.3	120.4 153.7	7.8 10.8	37	30
TS32-294†	60 90	29.8 78.6	375	108.5 295.5	98.0 279.9	5.4 13.1	40	34
TS32-588	60 70	68.5 89.6	400	246.4 330.8	243.4 303.7	11.4 15.8	37	63
TS32-735	60 70	66.7 90.0	380	240.8 332.4	198.4 276.4	7.7 11.3	37	63
TS32-0 (θ=22.5°)	90 100	43.9 52.0	400	172.8 186.7	180.7 187.6	6.1 6.5	64	42
TS32-0 (θ=30°)	110 120	41.4 65.0	400	166.9 261.5	173.2 267.1	4.5 8.2	89	45
T32-0 (Lm=125)	40 60	5.2 5.7	325	18.9 18.2	22.8 22.5	0.57 0.6	37	40
T32-0 (Lm=250)	80 120	62.6 123.5	450	258.1 509.4	233.9 457.3	22.4 47.7	37	38
T32-0 (Lm=300)	100 150	115.3 175.0	450	450.6 675.2	399.4 619.6	25.1 54.8	37	45
T32-0 (Lm=350)	120 150	118.1 140.0	475	471.7 557.3	406.7 535.3	42.2 73.8	37	39

† Reported previously by Guo and Qin (2010)

Table 3 Frame movement versus depth of moving soil

Block 1 (Final L_m= 200mm (15°))	Frame movement w_f (mm)	10	20	30	50	70	110	120	140
	Number of fully mobilized frames	2	3	4	6	8	8	8	8
	Depth of soil movement, mm	50	75	100	150	200	200	200	200
	Sliding depth ratio, R_L	0.07	0.10	0.14	0.21	0.29	0.29	0.29	0.29

Block 1 (Final L_m= 350mm (15°))	Frame movement w_f(mm)	60	70	80	90	100	110	120	140
	Number of fully mobilized frames	8	9	10	11	12	13	14	14
	Depth of soil movement, mm	200	225	250	275	300	325	350	350
	Sliding depth ratio, R_L	0.29	0.32	0.36	0.39	0.43	0.46	0.50	0.50
Block 2 (TS32-0 (θ=22.5°))	Frame movement w_f(mm)	20	30	40	50	70	80	90	110
	Number of fully mobilized frames	2	3	4	5	6	7	8	8
	Depth of soil movement, mm	50	75	100	125	150	175	200	200
	Sliding depth ratio, R_L	0.07	0.10	0.14	0.18	0.21	0.25	0.29	0.29
Block 3 (TS32-0 (θ=30°))	Frame movement w_f(mm)	30	40	60	70	90	100	110	120
	Number of fully mobilized frames	2	3	4	5	6	7	8	8
	Depth of soil movement, mm	50	75	100	125	150	175	200	200
	Sliding depth ratio, R_L	0.07	0.10	0.14	0.18	0.21	0.25	0.29	0.29

Figure Captions

Fig. 1 Schematic diagram of shear box
Fig. 2 Schematic of the triangular loading blocks
Fig. 3 Schematic test of a pile subjected to triangular loading block
Fig. 4 Responses of pile during test TS32-588
Fig. 5 Pile responses at varying distances of pile location (S_b=340, 500, 660mm, series 1)
Fig. 6 Pile responses under varying axial load levels (P=0, 294, 588,735N, series 2)
Fig. 7 Pile responses at different loading block angles (θ=15°, 22.5°, 30°, series 3)
Fig. 8 Pile responses at varying sliding depths (L_m=125, 200, 250, 300, 350mm, series 4)
Fig. 9 Variation of pile responses with distance S_b
Fig. 10 Soil movement surrounding pile at ground surface w_f = (a) 20mm; (b) 60mm; (c) 100mm; (d) 130mm
Fig. 11 Variation of pile responses with loading block angles
Fig. 12 Variation of M_{max} with wall rotation or loading block angle
Fig. 13 Varaition of M_{max} with sliding depth ratio R_L
Fig. 14 Maximum shear forces T_{max} versus maximum bending moments M_{max}
Fig. 15 Predicted and measured pile response (a) Prediction by design charts and full analysis (Chen and Poulos, 1997) (b) Maximum shear force versus maximum bending moment (c) calculation using current elastic solution
Fig. 16 Predicted and measured pile response (Lirer 2012) (a) Maximum shear force versus maximum bending moment (b) Maximum shear force versus ground surface displacement

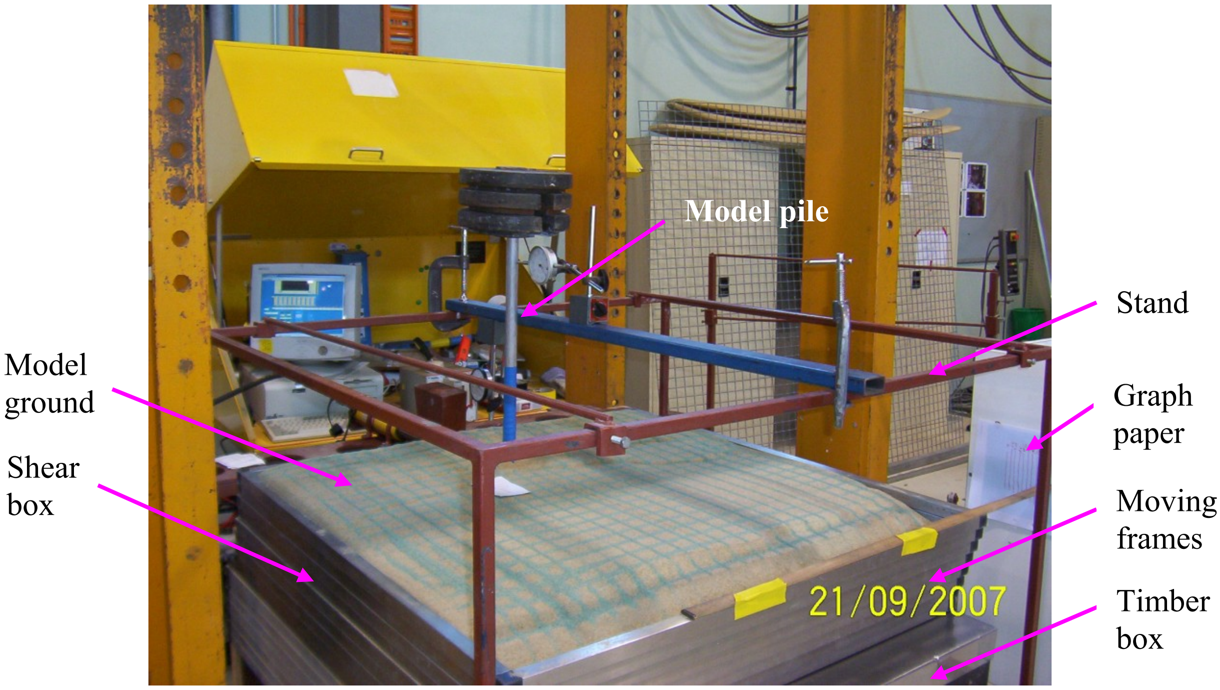

(a) Test setup

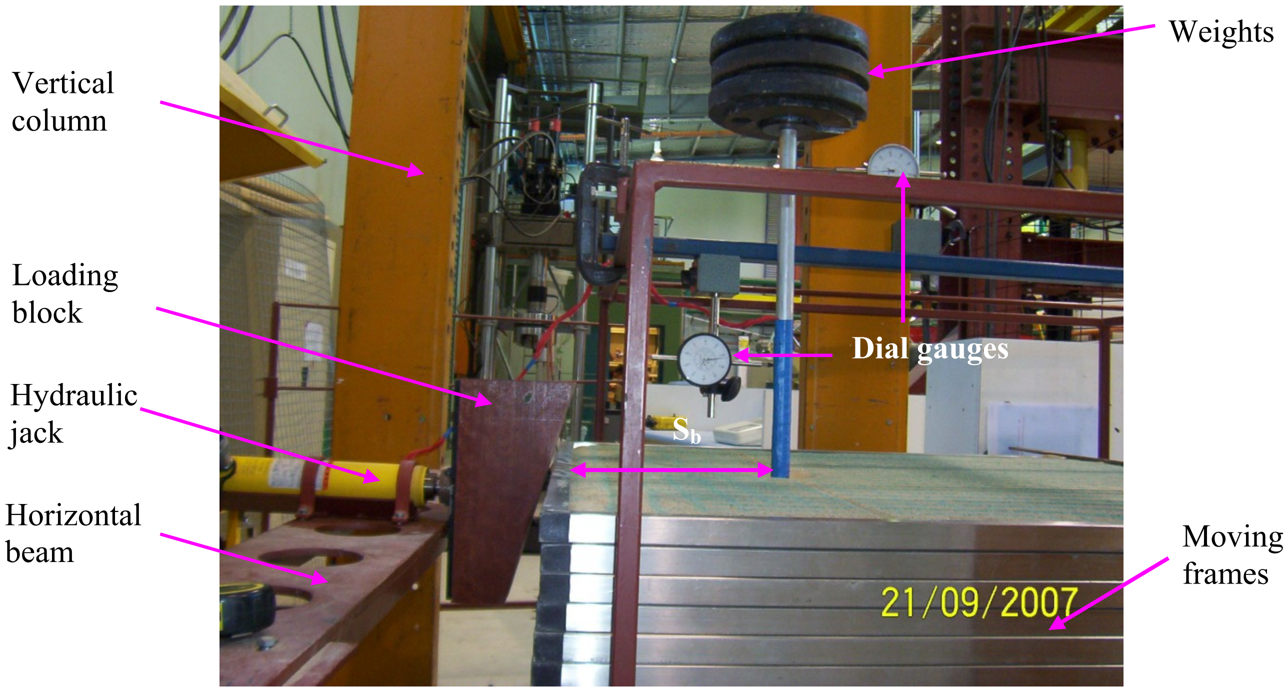

(b) Loading system

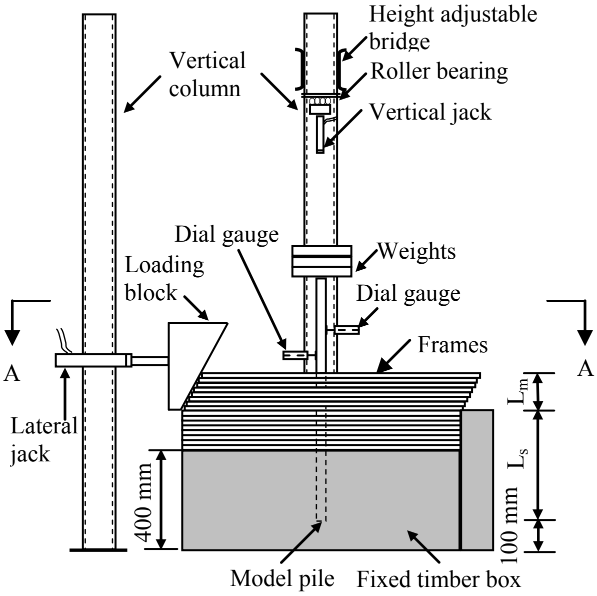

(c) Elevation view

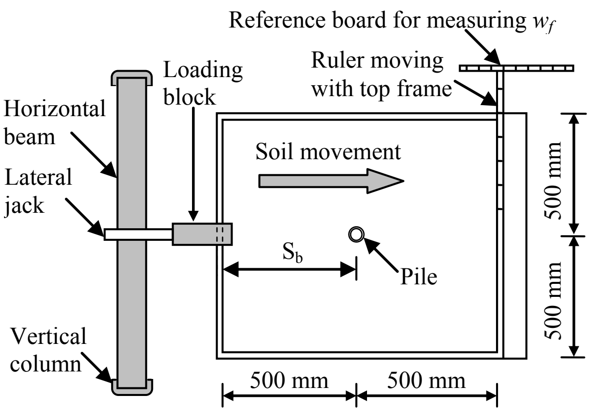

(d) Plan view (A-A)

Fig. 1. Schematic diagram of shear box

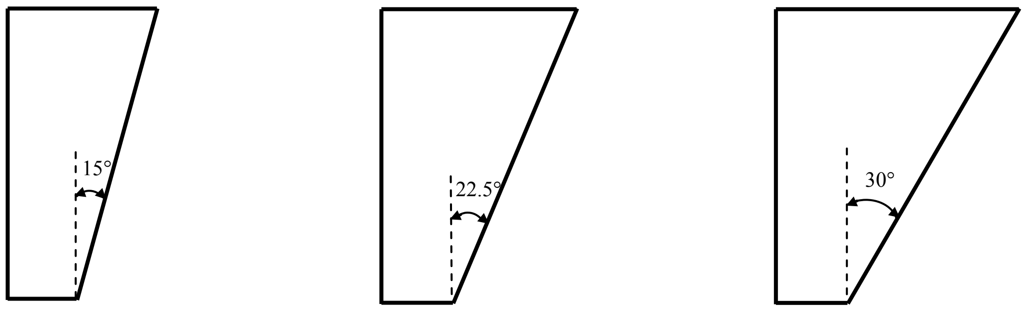

(a) block 1 **(b) block 2** **(c) block 3**

Fig. 2. Schematic of the triangular loading blocks

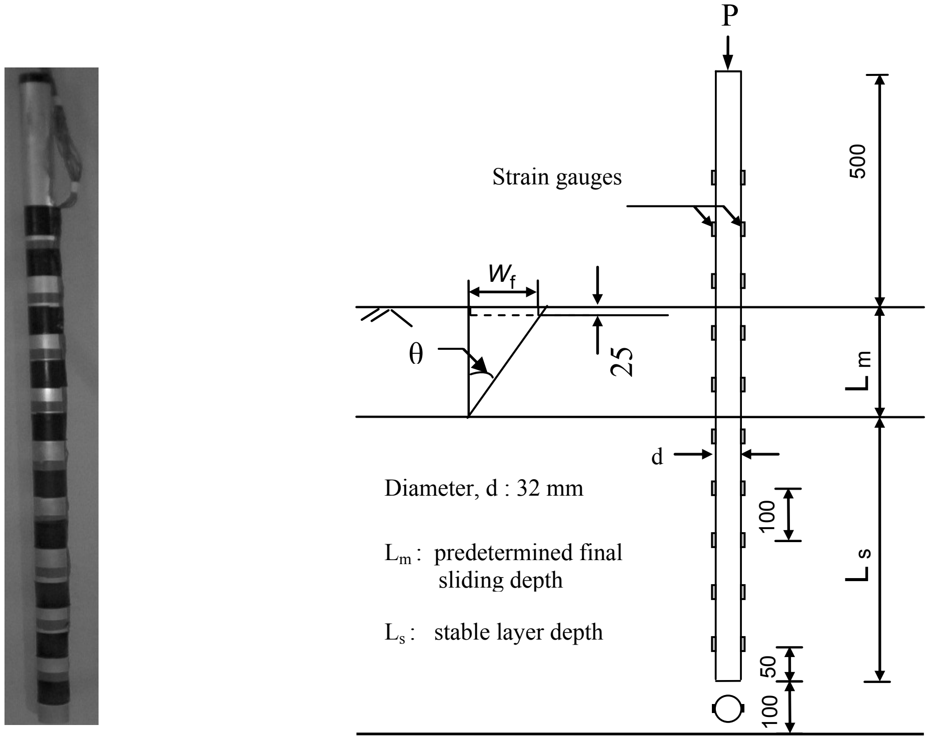

(a) An instrumented model pile **(b) Schematic diagram of testing**

Fig. 3. Schematic test of a pile subjected to triangular loading block

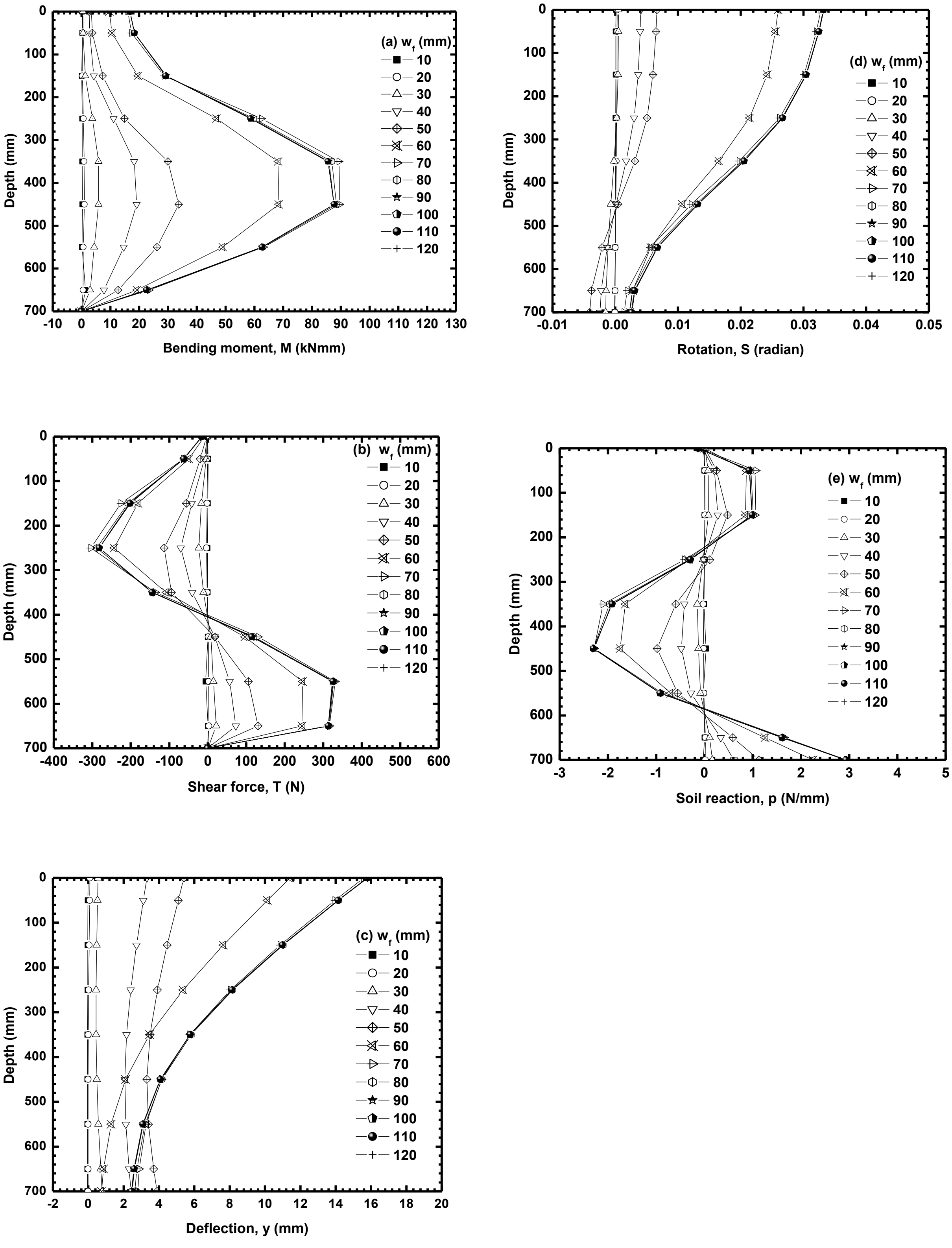

Fig. 4. Response of pile during TS32-588

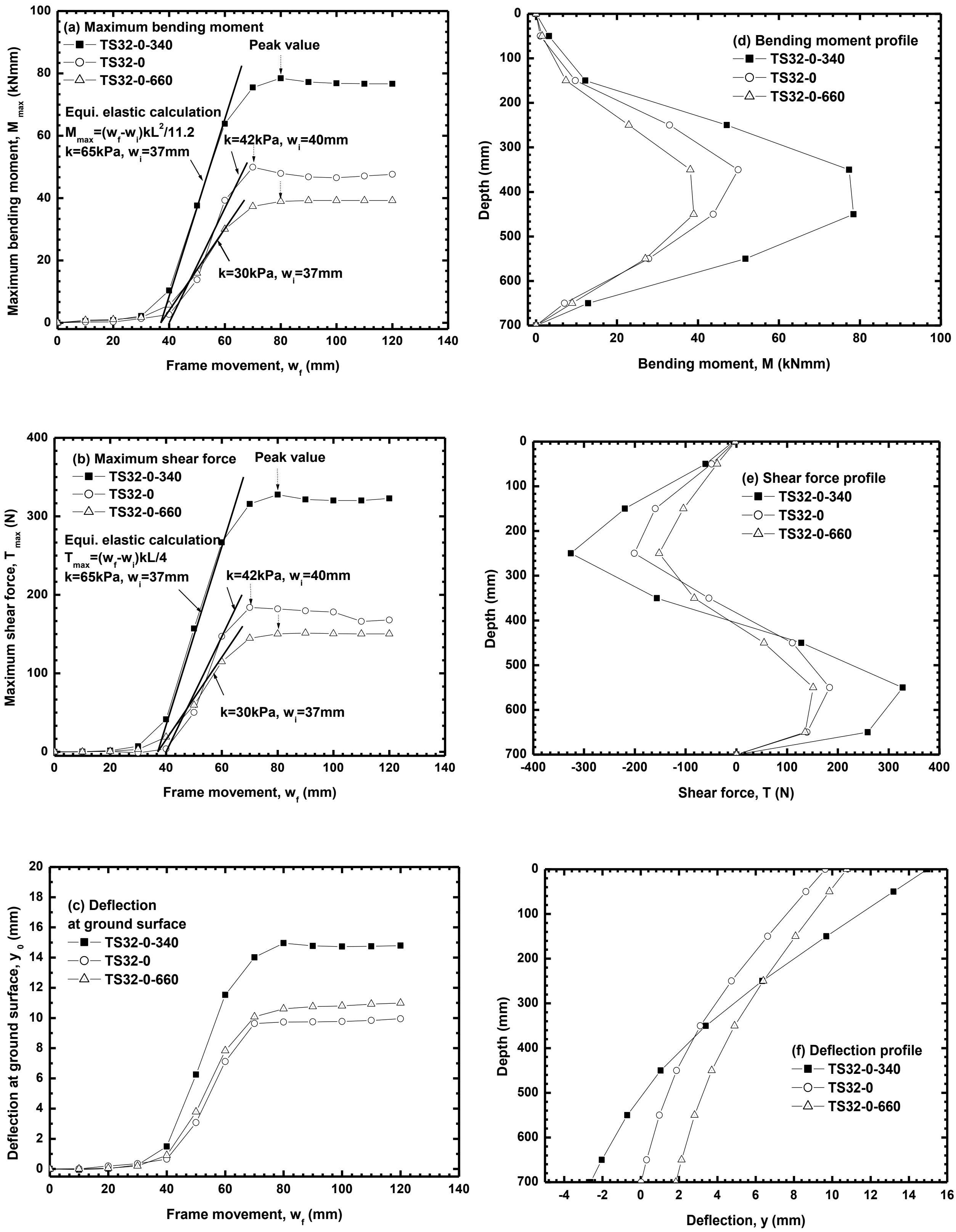

Fig. 5. Pile responses at varying distances of pile location (S_b = 340mm, 500mm, and 660 mm, series 1)

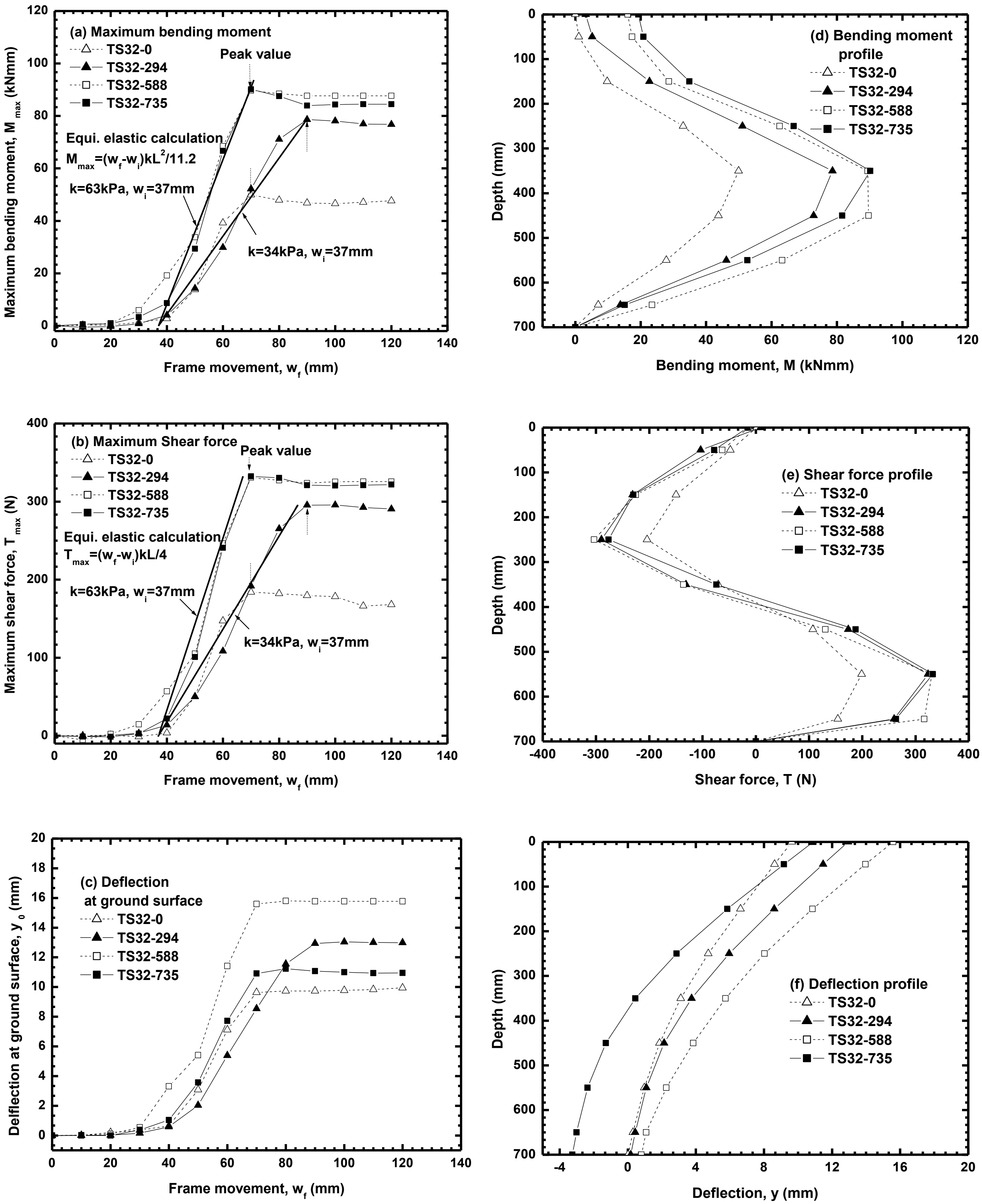

Fig. 6. Pile responses under varying axial load levels (P = 0 N, 294 N, 588 N, and 735 N, series 2)

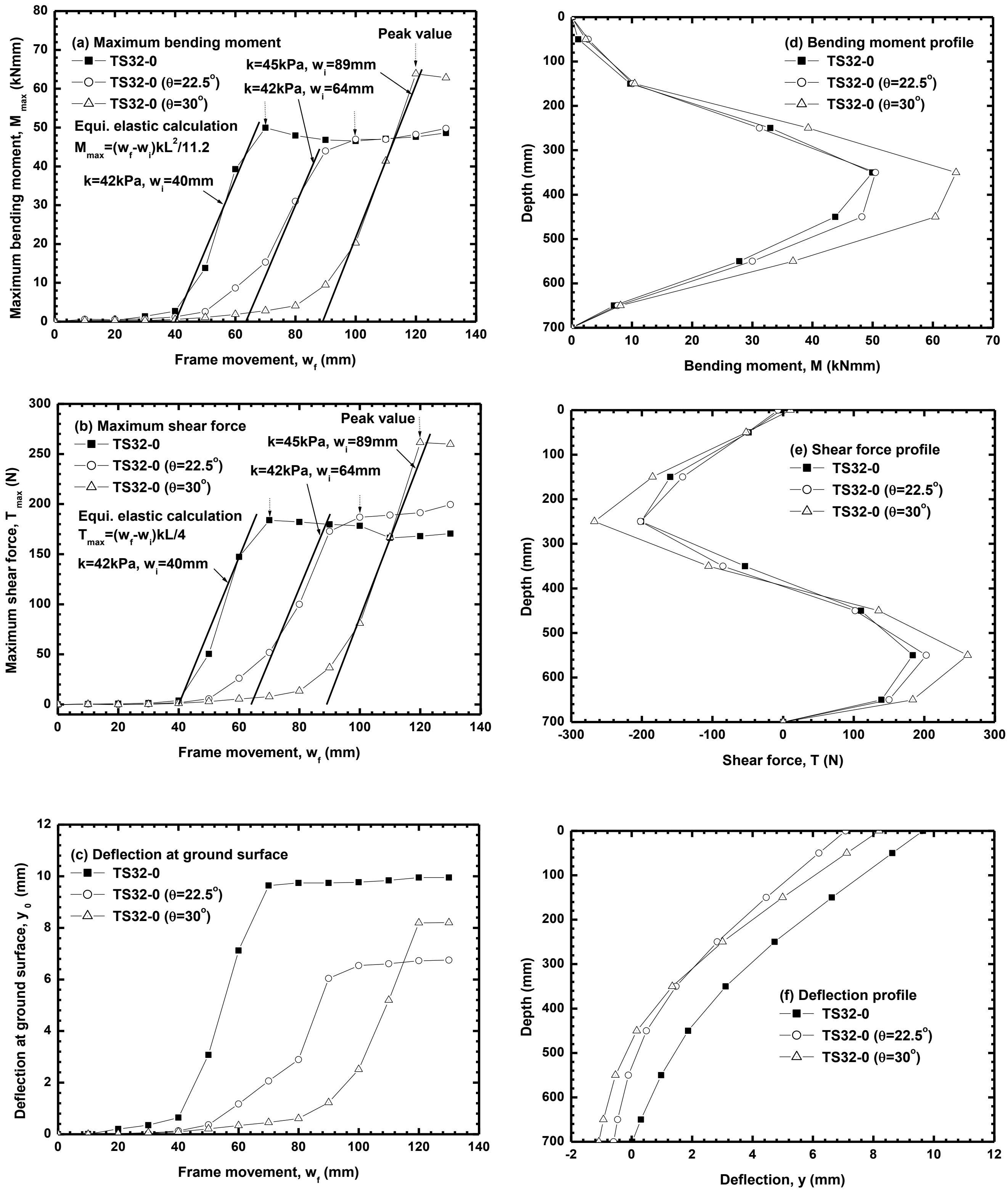

Fig. 7. Pile responses at different loading block angles (θ = 15°, 22.5°, and 30°, series 3)

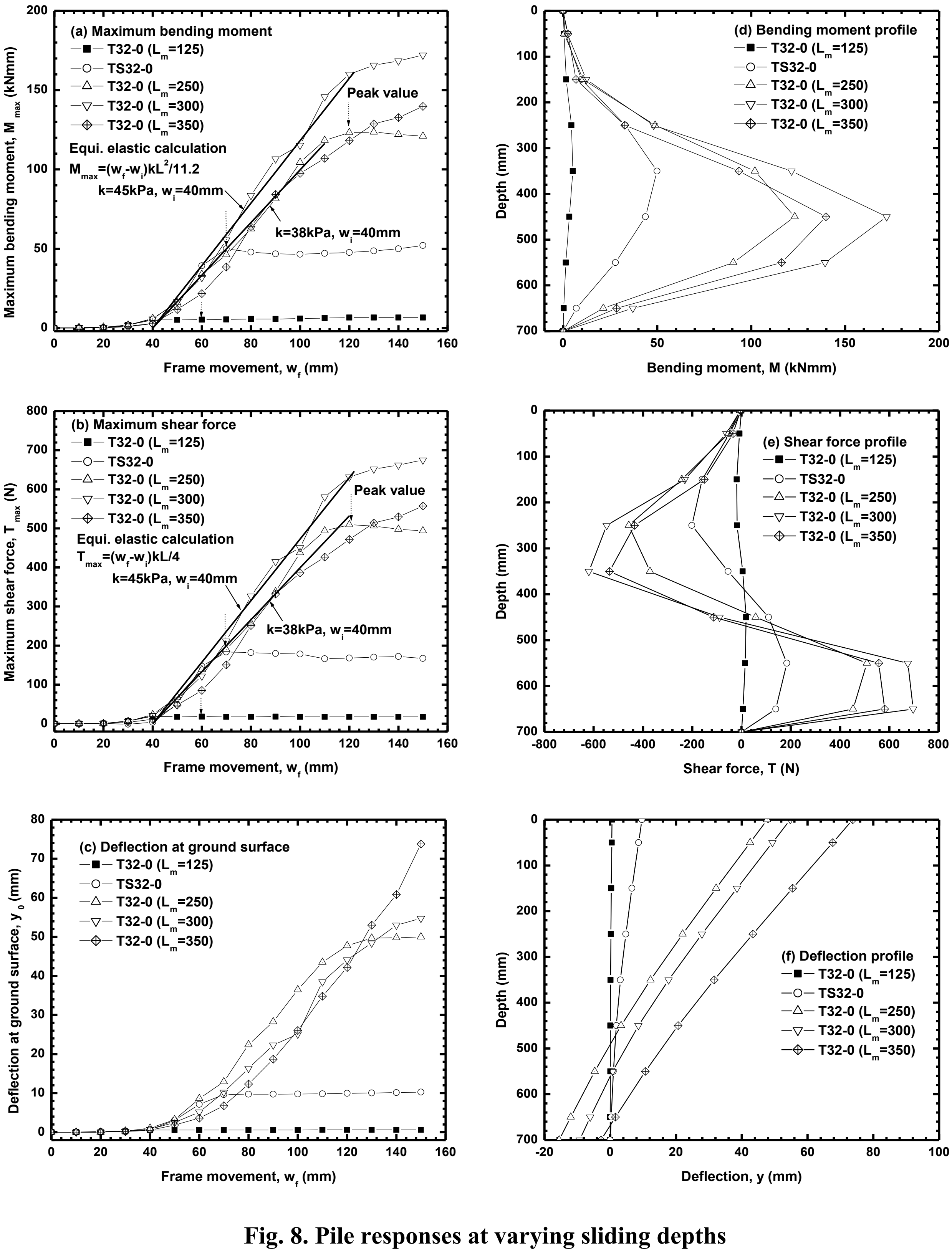

Fig. 8. Pile responses at varying sliding depths
(L_m = 125 , 200 , 250, 300, and 350 mm, series 4)

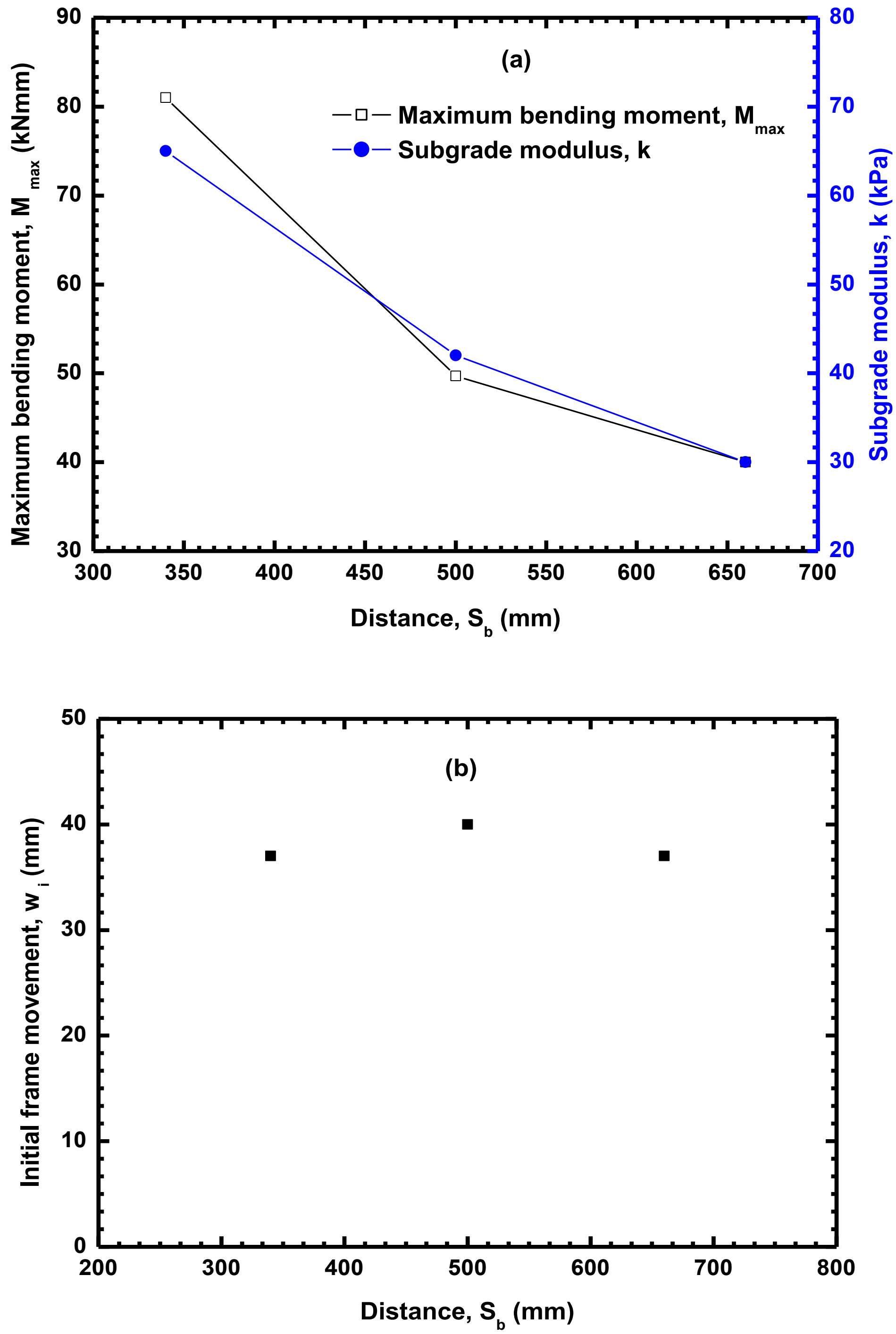

Fig. 9. Variation of pile responses with distance S_b

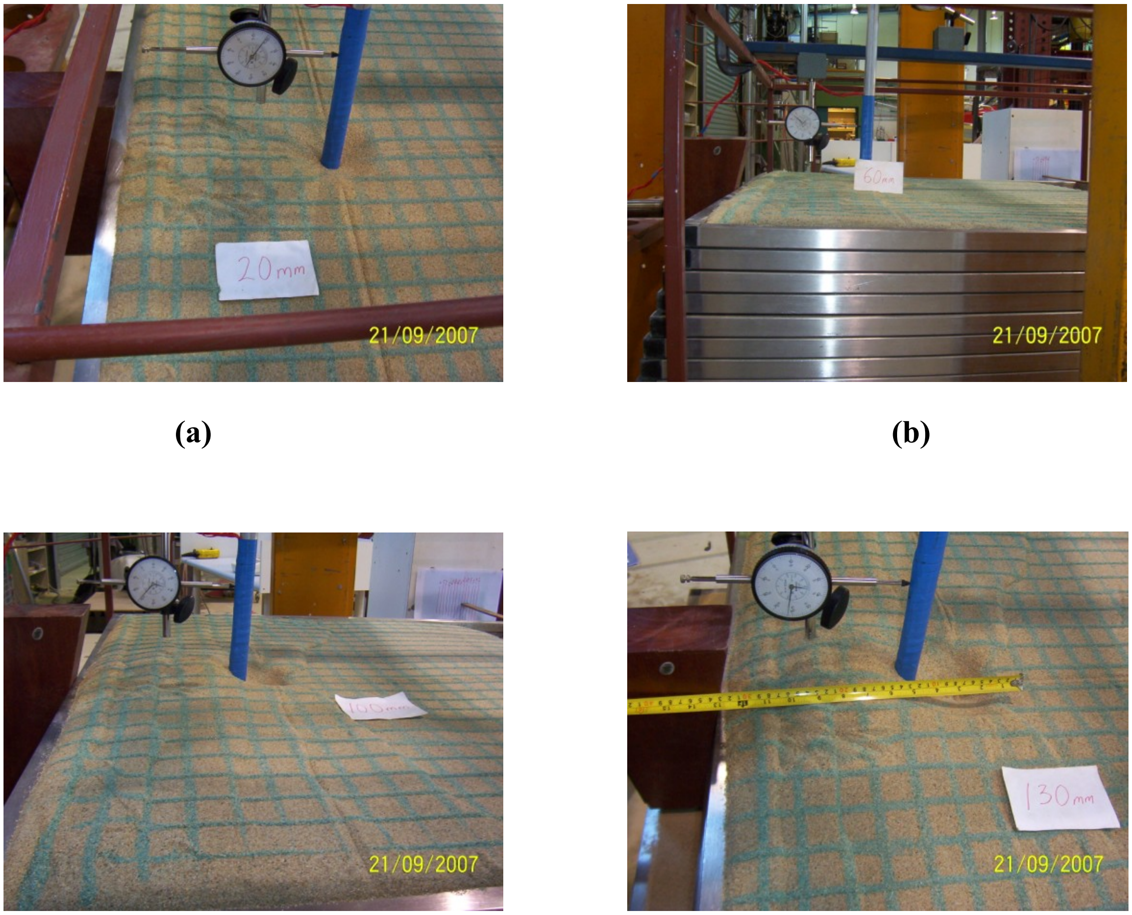

(a) (b)

(c) (d)

Fig. 10. Soil movement surrounding pile at ground surface
w_f = (a) 20mm; (b) 60mm; (c) 100mm; (d) 130mm

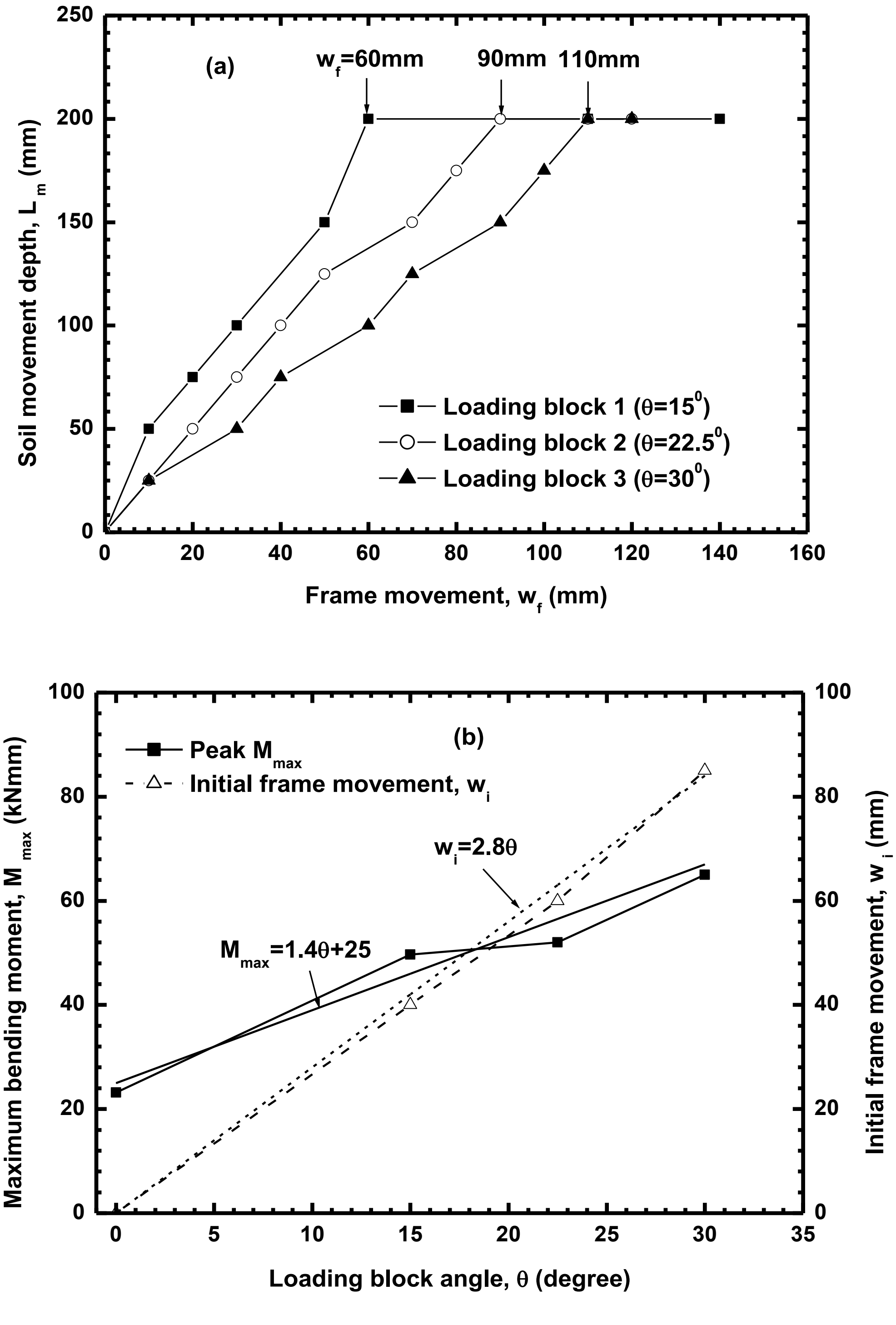

Fig. 11. Variation of pile responses with loading block angles

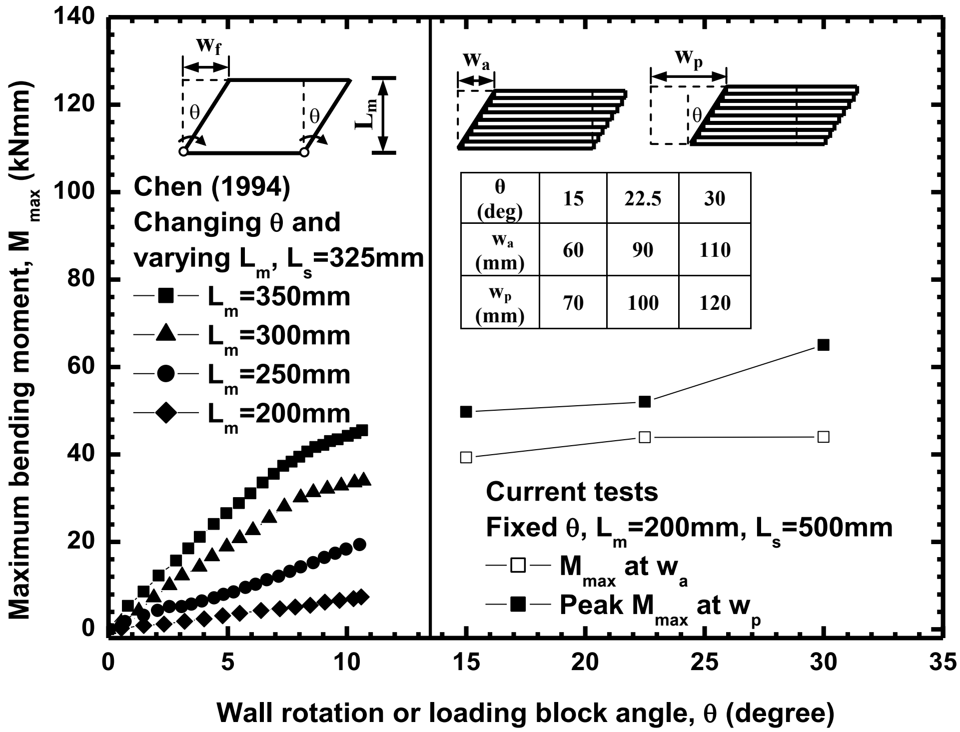

θ (deg)	15	22.5	30
w_a (mm)	60	90	110
w_p (mm)	70	100	120

Fig. 12. Variation of M_{max} with wall rotation or loading block angle

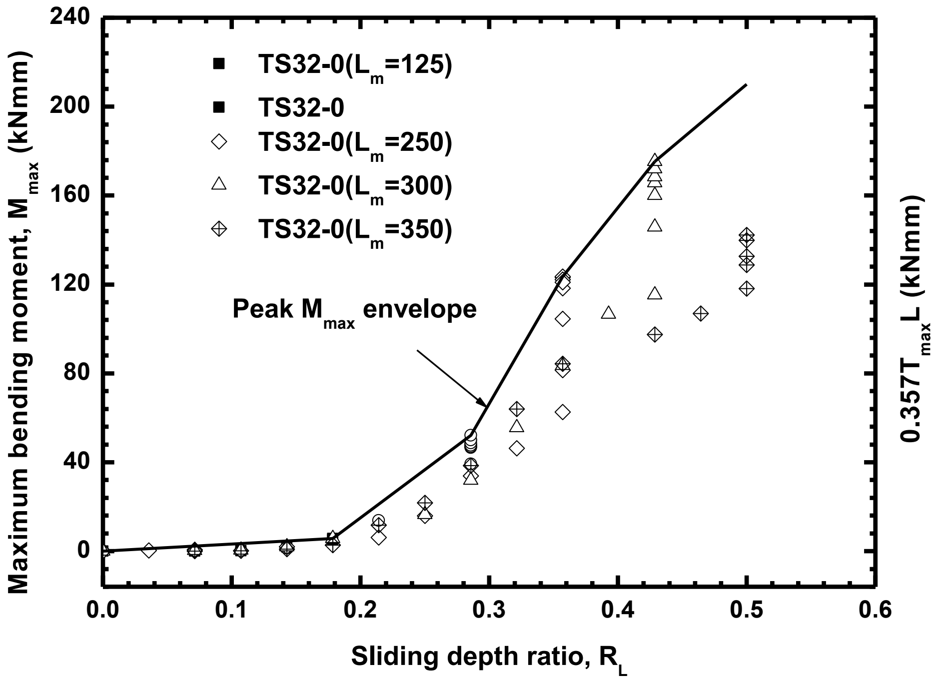

Fig. 13. Varaition of M_{max} with sliding depth ratio R_L

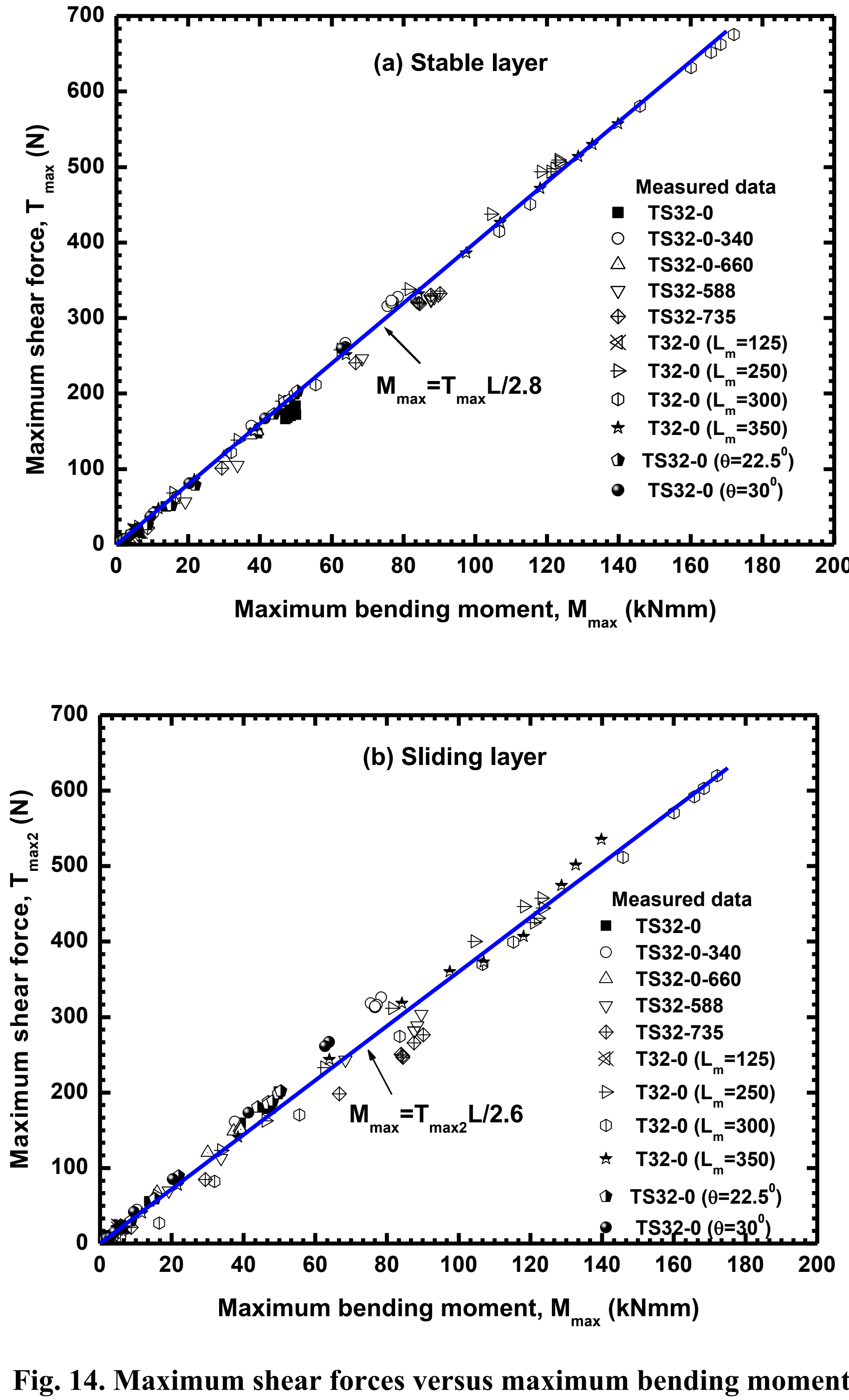

Fig. 14. Maximum shear forces versus maximum bending moments

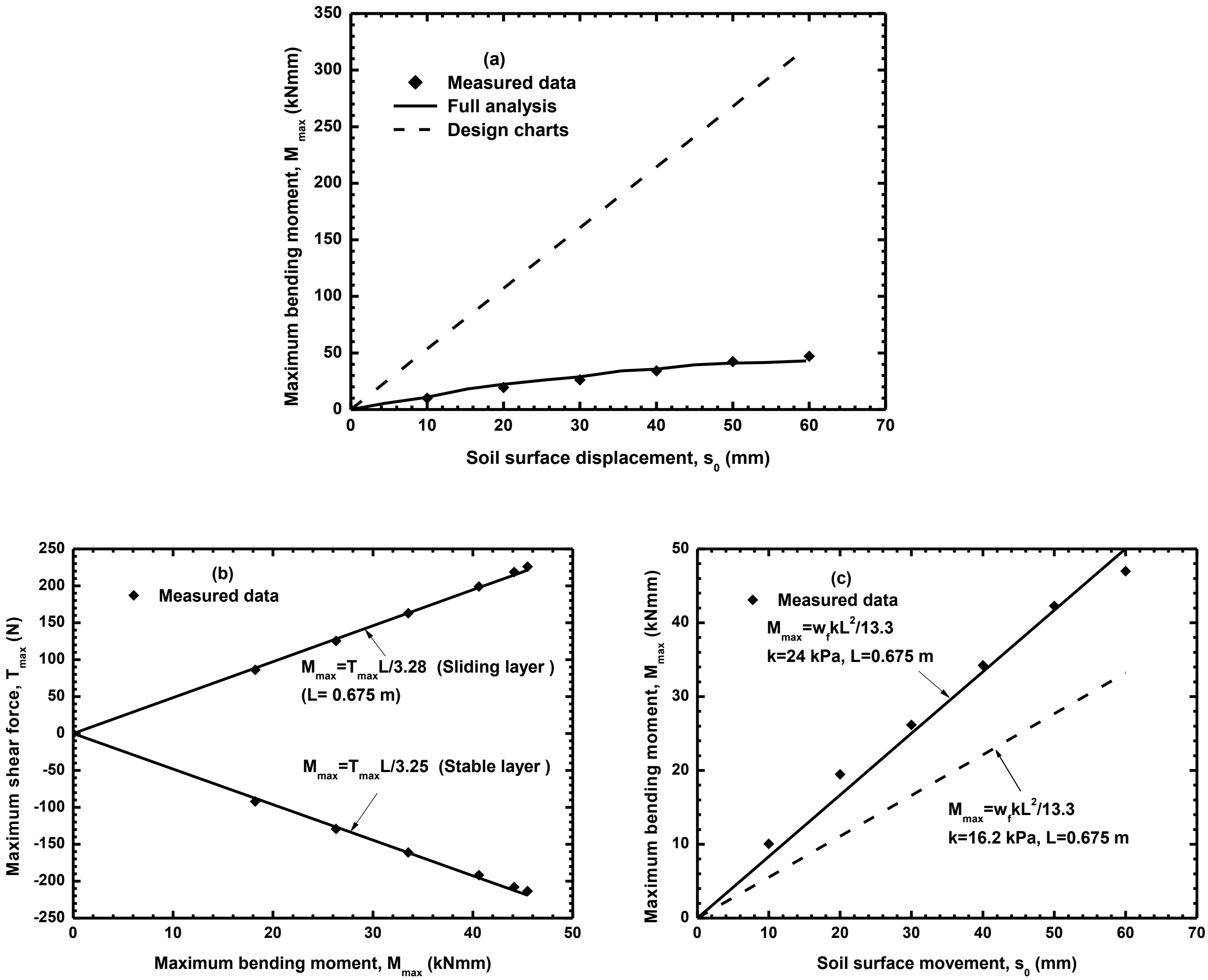

Fig. 15 Predicted and measured pile response
(a) Prediction by design charts and full analysis (Chen and Poulos, 1997) (b) Maximum shear force versus maximum bending moment (c) calculation using current elastic solution

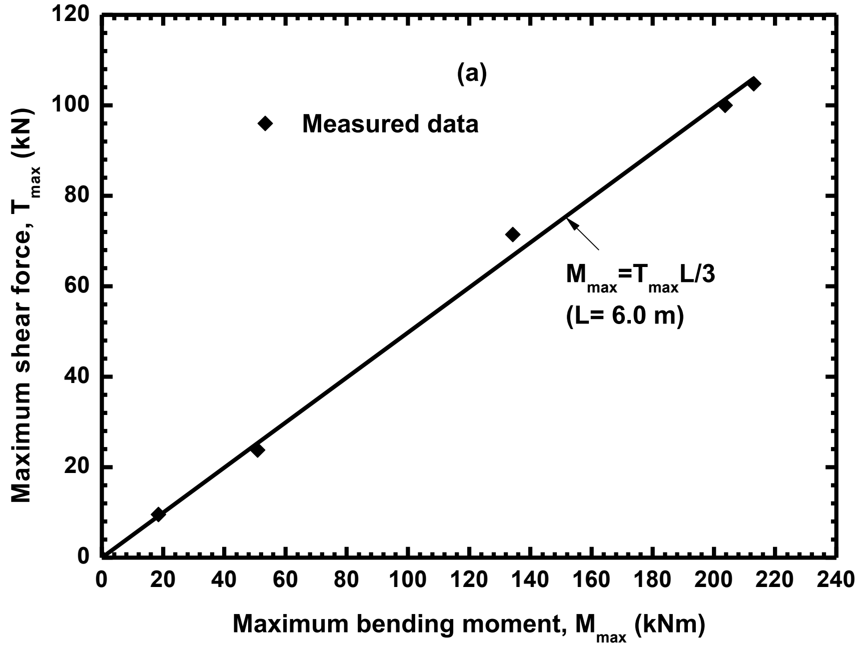

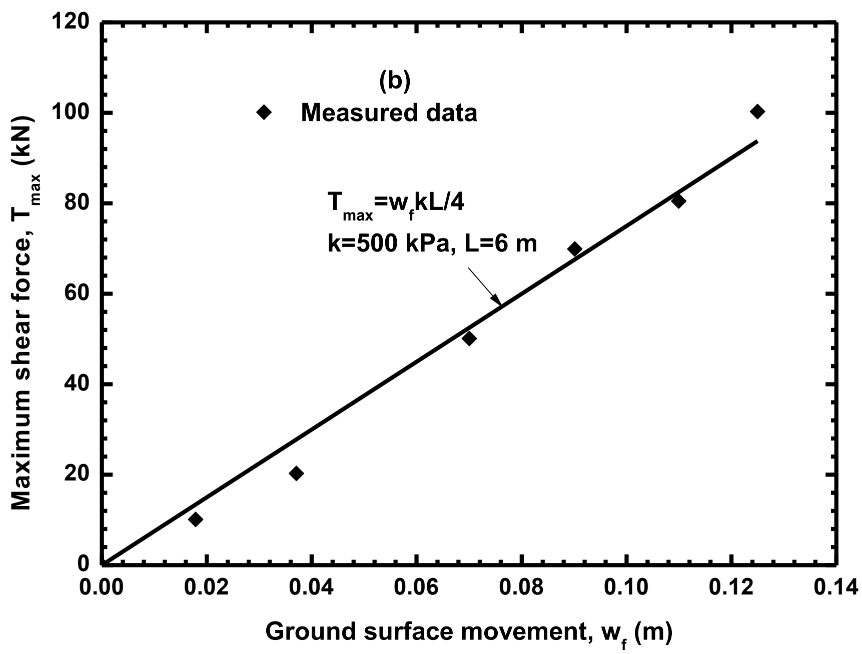

Fig. 16 Predicted and measured pile response (Lirer, 2012)
(a) Maximum shear force versus maximum bending moment (b) Maximum shear force versus ground surface displacement